

**Environmental Radiation Dose Rate in the Gold Mining Region of Lolgorian in  
Narok County**

**By**

Amos Kipkosgei Chepkwony (B.ED Physics)

A thesis submitted in partial fulfilment for the requirements for the award of degree of  
Master of Science in Nuclear Science of the University of Nairobi

**July 2018**

## **DECLARATION**

I hereby declare that this thesis is my original work and has not been submitted for the award of any degree or qualification at any other University.

Amos Kipkosgei Chepkwony, S56/73613/2014

Signature ..... Date .....

### **Supervisors' approval**

This thesis has been submitted with our knowledge and approval as university supervisors.

- 1) Mr Michael J. Mangala,  
Institute of Nuclear Science and Technology,  
University of Nairobi

Sign .....

Date .....

- 2) Dr. Geoffrey O. Okeng'o  
Department of Physics  
University of Nairobi

Sign .....

Date .....

## **DEDICATION**

Dedicated to my late parents Joseph and Pauline.

## **ACKNOWLEDGEMENT**

I wish to extend my gratitude to the Institute of Nuclear Science and Technology community for their support during my study period. I thank my supervisors; Mr. Michael Mangala (INST), Dr. Geoffrey Okengo (Physics Department) and Mr. Simon Bartilol, Senior technologist at the Institute of Science and Technology, University of Nairobi, for their support and guidance during my research period.

I thank the National Research Fund (NRF) for the research grant, I was awarded to facilitate this research study.

## ABSTRACT

Exposure to radiation leads to harmful health effects on human beings, either deterministic or stochastic depending on the threshold of the radiation dose. Knowledge on the radiation profile of a particular working environment should be a requirement to both the radiation regulatory authorities and the occupational workers. Currently there exists little to none radiological information on the gold mining region of Lolgorian. This study serves to bridge this gap in knowledge and data from the mining region.

This study was done in the gold mining region of Lolgorian in Narok County, specifically to determine radioactivity concentrations of thorium, potassium and uranium radionuclides, and to evaluate the associated radiation hazard indices. The study was done by analyzing thirty six (36) soil samples from Lolgorian for radioactivity measurements using hyper pure germanium detector.

The greatest contributor to radiation exposure in the vicinity of Lolgorian gold mines was  $^{40}\text{K}$ , with a mean activity concentration of  $427 \pm 116 \text{ Bq kg}^{-1}$  (74%), as compared to  $^{232}\text{Th}$  and  $^{238}\text{U}$  at  $116 \pm 69 \text{ Bq kg}^{-1}$  (20%) and  $33 \pm 22 \text{ Bq kg}^{-1}$  (5%) respectively. The  $^{238}\text{U}$  activity concentration was within the UNSCEAR global mean of  $35 \text{ Bq kg}^{-1}$ , while  $^{232}\text{Th}$  and  $^{40}\text{K}$  radionuclides were slightly above the global mean of  $30 \text{ Bq kg}^{-1}$  and  $400 \text{ Bq kg}^{-1}$  respectively. Radium equivalent values ranged between  $38 - 529 \text{ Bq kg}^{-1}$ , with a mean of  $232 \pm 38 \text{ Bq kg}^{-1}$ ; which is above the world mean reported at  $160 \text{ Bq kg}^{-1}$ , but within the UNSCEAR permissible limit of  $370 \text{ Bq kg}^{-1}$ . Gamma radiation index  $I_{\gamma r}$  was determined to have a mean of  $1.66 \pm 0.28$ , hence exceeding the required index value of unity ( $\leq 1$ ). Internal and external hazard index were determined to be  $0.72 \pm 0.14$  and  $0.62 \pm 0.11$  respectively.

The absorbed dose rates at 1 m distance above the ground level was determined at between  $19 \text{ nGy h}^{-1}$  and  $156 \text{ nGy h}^{-1}$ . The annual effective dose using an outdoor occupancy factor of 0.4 had a mean value of  $0.25 \pm 0.04 \text{ mSv y}^{-1}$ , which is below the mean global annual effective dose at approximately  $0.5 \text{ mSv y}^{-1}$ .

Fe was the major constituent in the soil samples, followed by Ti and Mn, with a mean concentration of  $9.22 \pm 7.70 \%$ ,  $4370 \pm 2500 \text{ mg kg}^{-1}$ , and  $1869 \pm 1509 \text{ mg kg}^{-1}$  respectively. Other mean concentrations below  $100 \text{ mg kg}^{-1}$ , were recorded for Zn, Zr, Rb and Pb. Zn concentrations ranged between  $(20 - 792) \text{ mg kg}^{-1}$ , with a mean of  $102 \text{ mg kg}^{-1}$ .

<sup>1</sup>. The study concluded that the radioactivity levels in the gold mining region of Lolgorian in Narok County currently do not pose significant risk to the public. However, there is need to analyze radioactivity levels in water sources to get a complete understanding of the extent of radioactivity distribution. Continuous periodic monitoring of the region's radionuclide concentration is recommended.

## **LIST OF ABBREVIATIONS AND ACRONYMS**

EPA	-	Environmental Protection Agency
H <sub>ex</sub>	-	External Hazard Index
H <sub>in</sub>	-	Internal Hazard Index
HPGe	-	High Purity Germanium Detector
IAEA	-	International Atomic Energy Agency
ICRP	-	International Commission on Radiological Protection
INST	-	Institute of Nuclear Science and Technology
NORMs	-	Natural Occurring Radioactive Materials
TENORM	-	Technologically Enhanced Naturally Occurring Radioactive Material
UNSCEAR	-	United Nation's Scientific Committee on the Effects of Atomic Radiation

## TABLE OF CONTENT

<b>DECLARATION</b> .....	<b>i</b>
<b>DEDICATION</b> .....	<b>ii</b>
<b>ACKNOWLEDGEMENT</b> .....	<b>iii</b>
<b>ABSTRACT</b> .....	<b>iv</b>
<b>LIST OF ABBREVIATIONS AND ACRONYMS</b> .....	<b>vi</b>
<b>TABLE OF CONTENT</b> .....	<b>vii</b>
<b>LIST OF TABLES</b> .....	<b>ix</b>
<b>LIST OF FIGURES</b> .....	<b>x</b>
<b>CHAPTER ONE: INTRODUCTION</b> .....	<b>1</b>
1.1 Research Background.....	1
1.2 Description of the Study Area .....	2
1.3 Statement of the Problem .....	3
1.4 Objectives .....	4
1.4.1 Main Objective .....	4
1.4.2 Specific Objectives.....	4
1.5 Justification of the Study .....	4
1.6 Scope of the Study.....	5
<b>CHAPTER TWO: LITERATURE REVIEW</b> .....	<b>6</b>
2.1 Overview .....	6
2.2 Natural Radioactivity in the Environment.....	6
2.2.1 Potassium-40 in the Environment.....	7
2.2.2 Uranium Decay Series and its Progeny Products.....	8
2.2.3 Thorium Decay Series and its Progeny Products .....	9
2.3 Radiological Studies.....	10
2.4 Environmental Impact of Gold Mining .....	14
<b>CHAPTER THREE: METHODOLOGY</b> .....	<b>15</b>
3.1 Overview .....	15
3.2 Sampling: Description of the Study Area.....	15

3.3 Sampling.....	17
3.4 Sample Preparation for Radioactivity Measurements and Trace Elements	
Determination. ....	17
3.5 Instrumentation of HpGe Gamma Spectroscopy and measurements .....	17
3.6 Radiological Data Analyses .....	20
3.6.1 Radium equivalent.....	20
3.6.2 Gamma Index .....	21
3.6.3 External Hazard Index .....	21
3.6.4 Absorbed dose .....	21
3.6.5 Annual Effective Dose .....	21
3.7 EDXRF Elemental Analyses .....	22
<b>CHAPTER FOUR: RESULTS AND DISCUSSION .....</b>	<b>23</b>
4.1 Overview .....	23
4.1 Activity Concentration .....	23
4.2 Radiation Hazard Indices .....	28
4.3 Elemental Concentrations.....	31
<b>CHAPTER FIVE: CONCLUSION AND RECOMMENDATIONS .....</b>	<b>37</b>
5.1 Conclusion.....	37
5.2 Recommendations .....	37
<b>REFERENCES .....</b>	<b>38</b>

## LIST OF TABLES

Table 3.1: Recommended energy lines for gamma-ray emitters of environmental samples (IAEA, 2003) .....	19
Table 4.1: Certified reference material activity concentrations and detection limits; IAEA-RGTh-1, IAEA-RGU-1 and IAEA-RGK-1 respectively .....	24
Table 4.2: Summary of the obtained activity concentrations in Bqkg <sup>-1</sup> .....	25
Table 4.3: Calculated radiation hazard indices .....	29
Table 4.4: Results of the analyses of IAEA-PTXRF09 certified reference material .....	32
Table 4.5: Elemental Concentrations in soils samples .....	34
Table 4.6: Inter-element Correlation matrix.....	36

## LIST OF FIGURES

Figure 1.1: Geological map of Lolgorian region, Narok County, Kenya .....	3
Fig. 2.1: Decay scheme of potassium-40 Source: <i>Pradler, et. al., 2013</i> .....	8
Figure 2.2: Uranium and Thorium decay series (WNA, 2009).....	9
Figure 3.1(a) : Kenyan map indicating the Kilimapesa mining area in Lolgorian, Source: <a href="http://www.goldplat.com/projects/kilimapesa-gold-kenya">http://www.goldplat.com/projects/kilimapesa-gold-kenya</a> .....	15
Fig 3.1(b): A map showing the mining blocks sampled in Lolgorian.....	16
Figure 3.2: The HpGe gamma spectrometer at the Institute of Nuclear Science & technology (INST) .....	18
Figure 4.1: Spectral data for the certified references and a typical sample.....	23
Figure 4.2: Sample wise distribution of activity concentration due to $^{238}\text{U}$ , $^{232}\text{Th}$ and $^{40}\text{K}$ from measured samples.....	25
Figure 4.3: Relative abundance of the radionuclides in soils.....	27
Figure 4.4: Correlation between the activity concentration of $^{238}\text{U}$ and $^{232}\text{Th}$ .....	27
Figure 4.5: Correlation between the activity concentration of $^{238}\text{U}$ and $^{40}\text{K}$ .....	28
Figure 4.6: Correlation between the activity concentration of $^{40}\text{K}$ and $^{232}\text{Th}$ .....	28
Figure 4.7: Variation of radium equivalent in the samples .....	29
Figure 4.8: shows the variation of gamma index in the samples .....	30
Figure 4.9: Variation of $H_{\text{ex}}$ & $H_{\text{in}}$ in the samples.....	30
Figure 4.10: Variation of absorbed dose rates in the samples.....	31
Figure 4.11: Variation of annual effective dose equivalent in the samples .....	31

## CHAPTER ONE: INTRODUCTION

### 1.1 Research Background

Radioactivity is a natural nuclear decay phenomenon which is associated to both artificial and natural radionuclides. Artificial radioactive sources include those from nuclear medicine and equipment, nuclear reactors, industrial process just to name a few. On the other hand, natural radioactivity sources contribute significant bulk of public radiation exposure that arise from terrestrial (primordial radionuclides) and extraterrestrial-cosmic origin. Based on these three categories; i.e. cosmic, primordial and artificial sources, there are over sixty natural radionuclides present in the environment (EPA, 2006). These radionuclides are found in rocks, soil, water, air, food, and even in living tissues and thus universally present hazardous risk.

Terrestrial radiation is the most significant of natural radiation sources, accounting to about 80 % of the annual radiation exposure (Watson et al., 2005). It mainly follows decay of naturally occurring radioactive materials (NORMs), commonly known as primordial radionuclides in all environmental materials such as rocks, soils, water, among others. In principle the term NORMs refers to  $^{232}\text{Th}$ ,  $^{40}\text{K}$ ,  $^{238}\text{U}$ , in addition to their radioactive decay daughter nuclides. Accordingly, the radiation dose levels associated with the NORMs is generally low and varies, though not significantly within locality but largely depend on concentration of the radionuclides, based on geological background and mineral composition. Thus, exposure to radiation from NORMs is usually of little public concern, except in cases of occupational exposures (IAEA, 2005) and where there is anomaly. However, even though the degree of exposure to NORMs is usually statistically insignificant from a medical physics perspective, the associated possible health risks cannot be ignored (World Nuclear Association, 2011).

In general exposure to ionizing radiation can result in an array of health effects both deterministic and stochastic. Deterministic effects result from acute radiation exposure above the threshold dose. It leads to death of cells, tissue or organ damage, and in unfortunate incidences, death. Examples of deterministic effects include loss of hair, nausea and vomiting. On the other hand, stochastic effects are probabilistic with no threshold dose. They can result from long term exposure to low radiation doses associated

with NORMs. These effects are specific to the organ exposed, dose rate, degree of absorbed dose and exposure period (UNSCEAR, 2000).

Virtually all soils and rocks contain NORMs to some degree, uranium and thorium are in very low concentrations (<0.1 %), while  $^{40}\text{K}$  is the most abundant in most natural environment. NORMs are found in very low concentrations, and their associated health risks usually considered negligible. However, anthropogenic activities such as mining, smelting, processing, milling etc., can result in elevated concentrations. Industrial processes such as mineral extraction result in high NORMs levels, commonly referred to as technologically enhanced naturally occurring radioactive materials (TENORM). The physical, chemical and radiological properties of the TENORMs are altered by being disturbed, beneficiated or processed, thus enhancing their potential for environmental exposure (EPA, 2008).

Mining activities have been known to result in the dispersion of the radionuclides at elevated concentrations. Therefore, this study seeks to determine radioactivity levels in Lolgorian gold mining areas in an effort to mitigate possible detrimental effects due to radiation exposure to both workers and the general public.

## **1.2 Description of the Study Area**

Lolgorian is a division in Narok County in Kenya, with its divisional headquarters being Lolgorian (1° 14' 0" S, 34° 48' 0" E). It borders Keyian, Kilgoris and Kirindon divisions and Mara triangle. The mining region lies between two rivers, river Mogor to the north and Mara River to the south. Lolgorian town is 364 Km south west of Nairobi and 265 Km from Nakuru and at altitude between 1156 m and 2278 m above sea level. The region experiences two rainy seasons; the short rains taking place September and December, while the long rains occur from March to June, with the wettest month being April. The climate of the region is classified as warm and temperate, the average temperature of the region being 17 degrees Celsius.

This study was conducted in the mining block SL91B that lies under the Migori greenstone belt. The geology of the study area is defined as Nyanzan basalts, with granite, greywacke Shales, tuffs, and Nyanzan Shales as the predominant underlying rocks. The region runs from Lake Victoria up to the late Proterozoic Mozambique belt to the east.

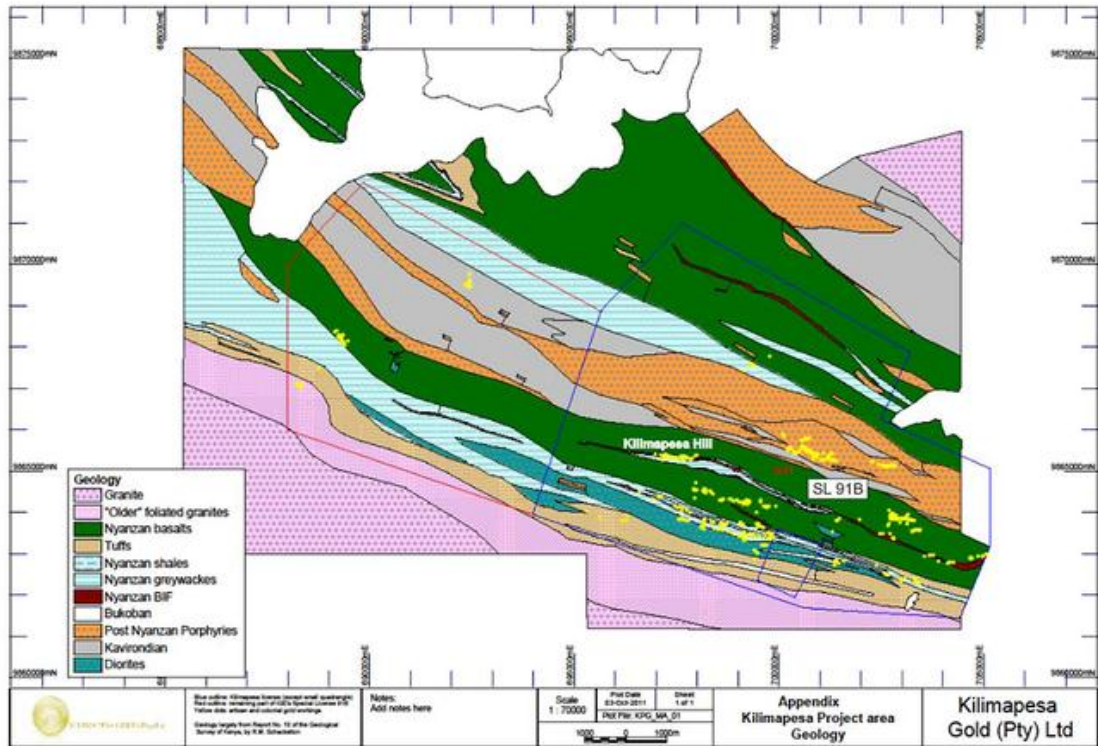


**Figure 1.1: Geological map of Lolgorian region, Narok County, Kenya**

### 1.3 Statement of the Problem

The contribution of the mining sector to a country's economy and development cannot be understated. To most of the global economies, this sector is actually a key foreign exchange earner. However, the mining sector has been associated with serious environmental concerns. Unfortunately, most studies and regulatory authorities focus on direct and more visible impacts such as soil and water contamination, erosion, loss of biodiversity, formation of sink holes, etc.

In general NORMs are associated to low health risks and are considered statistically negligible. However high concentrations have been reported in mining areas, and in high background radiation areas (Otwoma et al., 2012; Patel et al., 2012; Kinyua et al., 2001; Patel, 1991). The problem is further exacerbated during the mining processes which enhances (TENORMs). Such, could be the case in Lolgorian Gold mines, Kenya. In Lolgorian, the mining process entails deep ground excavation prior to extraction of

minerals, a process known to lead to elevated levels of natural radionuclides, which are hazardous to the mine workers and the public.

At the moment, there is no comprehensive data on the levels of radionuclide concentration and the extent of radiation exposures to both miners and the immediate environment of Lolgorian mines. This study therefore has profiled the environmental radiation exposure and is necessary in development of mitigation guidelines to minimise public exposure.

## **1.4 Objectives**

### **1.4.1 Main Objective**

To establish radiological hazards linked to natural radionuclides in Kilimapesa gold mines in Lolgorian, Narok County, Kenya.

### **1.4.2 Specific Objectives**

- i. To determine the activity concentrations of  $^{40}\text{K}$ ,  $^{232}\text{Th}$  and  $^{238}\text{U}$  in soil samples;
- ii. To estimate the absorbed dose rate and the annual effective dose rate in the collected soil samples;
- iii. To estimate the radium dose equivalent in the soil samples;
- iv. To determine the external and internal radiation hazard indices in the soil samples.

## **1.5 Justification of the Study**

Exposure to hazardous natural radionuclides can be harmful to human health in both short term and long term, based on the degree and duration of radiation exposure. Consequently, sufficient data on the radiation levels should not only be a requirement but a necessity for miners, the public and the relevant decision-making government agencies. This study therefore serves to bridge the knowledge gap on Lolgorian gold mines with respect to radionuclide concentration levels and the associated radiological hazards in the Lolgorian gold mines.

As such, the study will contribute towards public awareness creation on potential health hazards associated with radiation exposures and will in addition provide baseline data for future mitigation measures.

## **1.6 Scope of the Study**

This study is relevant for radiological protection and safety in Kilimapesa Gold mines and its immediate environs. The study is limited to identifying and quantifying the radionuclides ( $^{40}\text{K}$ ,  $^{238}\text{U}$  and  $^{232}\text{Th}$ , and their daughter progenies) activity concentrations in sub-soil samples collected from Kilimapesa mines and the estimation of radiological hazards. Absorbed dose was determined at 1m distance above the ground level considered the average height of a person. Other radiation exposure parameters; radium equivalent, annual effective dose, gamma index, and external and internal hazard indices were determined using existing models. The results obtained were used to determine the extent of environmental radiological contamination resulting from the mining processes

## CHAPTER TWO: LITERATURE REVIEW

### 2.1 Overview

This chapter presents a review and discussion on natural radioactivity and radionuclides in the environment followed by a review of past and recent studies on environmental radioactivity and dose rate assessments in support of the current study. The literatures cited in this chapter are purely from primary sources

### 2.2 Natural Radioactivity in the Environment

There are two categories of natural radioactivity; terrestrial and extra-terrestrial/cosmic radiation. Terrestrial radiation emanates from radionuclides contained in the earth's crust i.e. soil, minerals and rocks. It comprises of alpha and proton particles, whose interaction in the upper atmosphere leads to creation of secondary particles such as muons, electrons, neutrons and protons (UNSCEAR, 2000). Cosmic radiation on the other hand penetrates into the earth's atmosphere from the outer space i.e. galaxies and sun (Choppin et al, 2002). Interaction of cosmic rays with the constituent nuclei in the atmosphere results into a cascade of interactions and cosmogenic radionuclides. The most common cosmogenic radionuclides are  $^{14}\text{C}$  and  $^3\text{H}$ . With respect to dose from NORMs, the contribution of these radionuclides is insignificant due to attenuation in the atmosphere (UNSCEAR, 2008).

However, modification of the natural environment could result in higher radiation exposure from natural radionuclides. For example, human activities such as mining and use of rocks as key construction material expose human beings to elevated radiation doses, use of fossil fuel and phosphate fertilizers are other such activities that can alter the radiation levels in the environment (UNSCEAR, 2008).

In principle radiation exposure can either be internal or external, internal exposure results from ingestion or inhalation of radionuclides. On the other hand, external exposure can further be classified as outdoor and indoor exposure originating from the presence of NORMs in rocks, soil and minerals. The degree of exposure to outdoor exposure varies with the parent rock material from which the soil was derived. For instance, igneous rocks are associated with higher degree of radiation, whereas sedimentary rocks exhibit characteristically low degree of radiation. Phosphates and shales also exhibit higher concentration level of natural radionuclides (UNSCEAR, 2008). Indoor exposure results primarily from building materials such as sand, cement, stone, soil and bricks. A study by

Maina et al., (2002) observed that more than half of mud constructed houses in coastal Kenya exceeded the IAEA action level of  $200 \text{ Bq m}^{-3}$ , with some as high as  $400 \text{ Bq m}^{-3}$ . Radon was identified as the most common radiological indoor pollutant.

According to UNSCEAR (2008), gamma dose rate in air exhibits substantial temporal variations. This observation has been attributed mainly to radon, which is greatly affected by soil moisture content, snow or rainfall. Variations as high as 50 % have been recorded within a thirty-minute time interval. Increased gamma dose levels of (50 – 100) % lasting for several hours can be caused by rainfall or washout of the radon progeny. Subsequent decline can be associated with increased moisture content (UNSCEAR, 2008).

There are two categories of naturally occurring radionuclides; those that are radioactive in their own nature i.e. singly occurring radionuclides such as  $^{40}\text{K}$ ,  $^{50}\text{V}$ ,  $^{113}\text{Cd}$ ,  $^{142}\text{Ce}$ , etc., and those that belong to decay of nuclides i.e. uranium, actinium, thorium and neptunium decay series. Radioactive decay occurs in heavy nuclides ( $A > 209$ ;  $Z > 90$ ), either by beta emission resulting in a unit change in atomic number or by emission of alpha particles leading to a stepwise decline in mass number by 4. This decay process terminates once a stable nuclide is attained i.e.  $^{206}\text{Pb}$ ,  $^{207}\text{Pb}$  and  $^{208}\text{Pb}$  for  $^{238}\text{U}$ ,  $^{235}\text{U}$  and  $^{232}\text{Th}$  decay series, and  $^{209}\text{Bi}$  for  $^{237}\text{Np}$  decay series.

### **2.2.1 Potassium-40 in the Environment**

The isotopic abundance of  $^{40}\text{K}$  is 0.012 %. It has a half-life of approximately  $1.25 \times 10^9$  years. While  $^{39}\text{K}$  is an essential nutrient in animals and plants,  $^{40}\text{K}$  is a significant source of internal and external human radiation exposure. In general, the specific activity of natural  $^{40}\text{K}$  has specific activity of  $31.4 \text{ Bq/g}$ . The mean activity concentration of  $^{40}\text{K}$  in earth's crust is  $840 \text{ Bq/kg}$  and  $60 \text{ Bq/kg}$  in human body, its concentration in soils can be enhanced through agricultural activities like use of phosphate bearing fertilizers (Ajmalet al., 2014; Jibiri and Fasae, 2012). In terms of internal human exposure,  $^{40}\text{K}$  comes second after radon and its daughter products. According to a report by International Commission on Radiological Protection (ICRP, 1976),  $^{40}\text{K}$  is present in all biological systems, with an adult (70 Kgs) containing approximately 140g of potassium that translates to  $4.3 \text{ kBq}$  of  $^{40}\text{K}$  in the body, especially in the muscles.

$^{40}\text{K}$  has three modes of decay; positron emission, K-electron capture and  $\beta$  emission (Figure 2.1). The probability of positron emission is 0.0011 %, where a proton in the nuclide

decays into a positron, resulting into a change from  $^{40}\text{K}$  into  $^{40}\text{Ar}$  (Read and Hayder, 2011). In the second mode, that is K-electron capture,  $^{40}\text{K}$  nuclide decays indirectly into the stable state of  $^{40}\text{Ar}$  in two phases; first, into the excited state of argon; which then decays into its stable state via emission of gamma radiation of 1.46 MeV energy. The probability of occurrence of electron capture is 11 % (Read and Hayder, 2011). Lastly,  $^{40}\text{K}$  radionuclide can decay via emission of a  $\beta$ -particle into the stable state of  $^{40}\text{Ca}$ . The emitted  $\beta$ -particle has 1.32 MeV energy with probability of occurrence at 88.7 %, as the predominant mode (Read and Hayder, 2011).

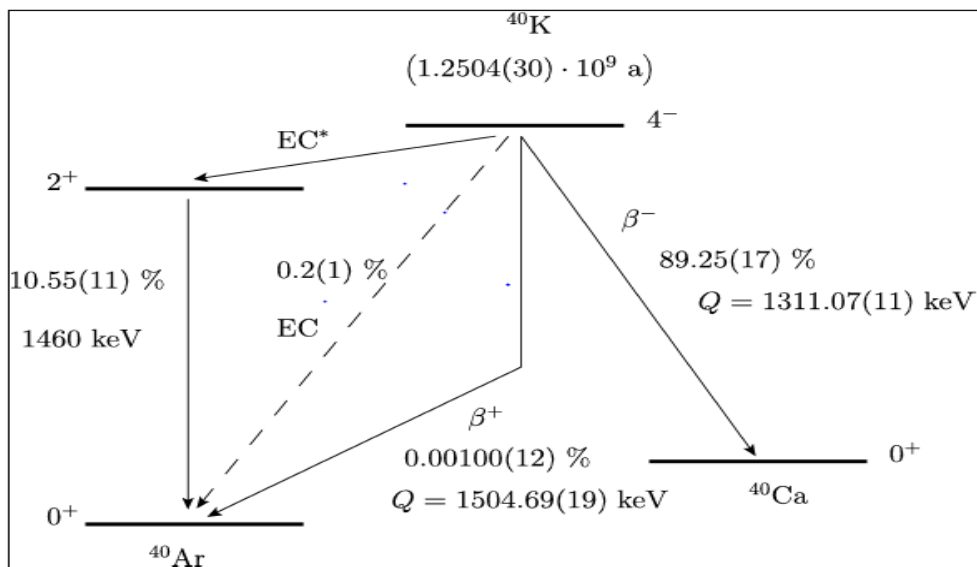


**Fig. 2.1: Decay scheme of potassium-40 Source: Pradler, et. al., 2013**

### 2.2.2 Uranium Decay Series and its Progeny Products

There are three isotopes of uranium atom;  $^{238}\text{U}$ ,  $^{235}\text{U}$ , and  $^{234}\text{U}$ . Uranium-238 is the most dominant at 99.3%, followed by  $^{235}\text{U}$  (0.72%) and  $^{234}\text{U}$  at 0.005% (Cember, 2009). Both  $^{238}\text{U}$  and  $^{234}\text{U}$  belong to  $4n+2$  series, that is, uranium series, while  $^{235}\text{U}$  belong to  $4n+3$  series (actinium series). Uranium decay series starts at  $^{238}\text{U}$ , and has a long half-life of  $4.5 \cdot 10^6$  years. In the process, fourteen nuclides are produced following emission six beta particles and eight alpha particles until a stable isotope of  $^{206}\text{Pb}$  is achieved (Figure 2.1) in addition to gamma radiation emissions. Among the decay products,  $^{214}\text{Bi}$  and  $^{214}\text{Pb}$  can readily be measured using gamma spectrometry. Due to a shorter half-life of the daughter products than the parent nuclide, uranium series is said to be in secular equilibrium

(Richard and Martin, 1997). On the other hand,  $^{235}\text{U}$  belongs to  $4n+3$  (Actinium) series, commencing at  $^{235}\text{U}$  and terminates at  $^{207}\text{Pb}$ , this decay series results in twelve nuclides and emission of seven alpha particles.

### 2.2.3 Thorium Decay Series and its Progeny Products

According to Australian Radiation Protection and Nuclear Safety Agency (ARPANSA, 2015) fact sheet, there are twenty-six known thorium isotopes. Among them, only twelve have half-life of more than a second and three with half-lives long enough to raise environmental concern i.e.  $^{232}\text{Th}$ ,  $^{230}\text{Th}$  and  $^{229}\text{Th}$ . However,  $^{232}\text{Th}$  is the most common (almost 100%) and significant of these natural radioisotopes and is the parent member of thorium ( $4n$ ) series. Thorium series involves ten decay phases with six alpha particles being emitted (Figure 2.2). Four of the resultant nuclides i.e.  $^{212}\text{Pb}$ ,  $^{228}\text{Ac}$ ,  $^{208}\text{Tl}$  and  $^{212}\text{Bi}$ , can readily be measured using gamma spectroscopy (Read and Hayder, 2011; Harb et al, 2008). According to Harb et al. (2008), for  $^{208}\text{Tl}$  to be used in estimating thorium activity, the obtained measurement must be corrected for branching during decay of  $^{212}\text{Bi}$  into  $^{212}\text{Po}$  by  $\beta$ -decay (64%) and  $^{208}\text{Tl}$  by  $\alpha$ -decay.

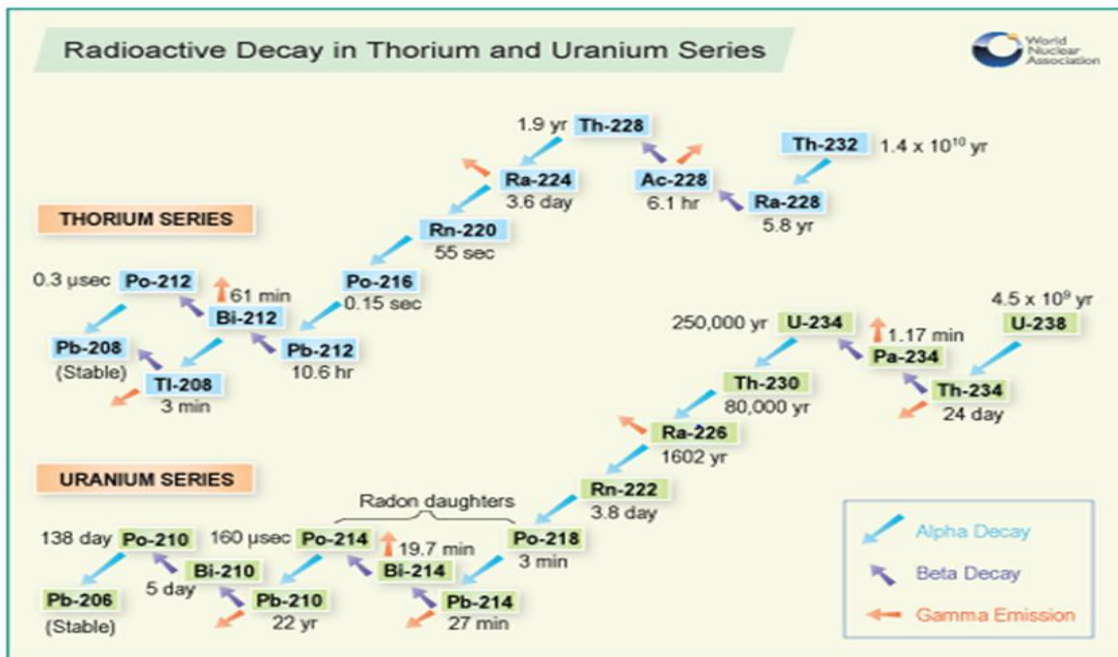


Figure 2.2: Uranium and Thorium decay series (WNA, 2009)

The most significant decay products in  $^{232}\text{Th}$ ,  $^{238}\text{U}$  and  $^{235}\text{U}$  series in terms of human exposure are the isotopes of radon ( $^{222}\text{Rn}$ ,  $^{220}\text{Rn}$ ,  $^{219}\text{Rn}$ ) and radon daughters, mainly  $^{210}\text{Po}$  and  $^{210}\text{Pb}$  (UNSCEAR, 2000; Richard and Martin, 1997). Radon isotopes,  $^{222}\text{Rn}$ ,  $^{220}\text{Rn}$ ,  $^{219}\text{Rn}$  results from an alpha decay of the radium isotopes  $^{226}\text{Ra}$ ,  $^{224}\text{Ra}$ ,  $^{223}\text{Ra}$  respectively. Radon is present in soils, rocks, water and air at varying concentrations. This is dependent mainly on soil and bedrock composition. Other factors that influence radon concentration are grain size and shape, geology of soil formation, soil permeability, temperature moisture content and radium concentration. For instance, for a mean radium concentration of  $40\text{Bq kg}^{-1}$ , the resultant radon concentration estimate is  $60\text{ Bqm}^{-3}$ . The action level for radon is  $1000\text{ Bq m}^{-3}$  for working area, based on 2000 hours occupancy level per year (ICRP, 2007). According to UNSCEAR (2000), the dominant radiological exposure pathway in human beings is through inhalation of radon and its progeny. This exposure is associated with alpha particles released by short-lived progeny of  $^{222}\text{Rn}$  and  $^{220}\text{Rn}$  radionuclides, deposited along the airways and lungs. The report further links irradiation of basal and secretory cells in the upper airways to lung cancer, especially underground miners (UNSCEAR, 2000). In United States, indoor radon exposure is estimated to cause approximately 20,000 lung cancer deaths annually (EPA, 2000).

### **2.3 Radiological Studies**

Radiation exposures resulting from the extraction and processing of minerals is an issue of public concern. Consequently, numerous studies have been conducted in Kenya, as well as globally, on radiological assessment in the mines. According to UNSCEAR (1993), the typical annual effective dose globally resulting from the extraction and refining of minerals, is estimated at  $20\text{ mSv/ year}$ . As a result, there has been an increase in number of radiological studies being conducted globally within the mines, suspected high background radiation areas, as well as recreational and residential areas such as beaches (Ademola, 2015; Sivakumara et al., 2014; Mustapha et. al., 2007; Darko et al., 2005). From such studies, there has been enhanced understanding of radiological hazards posed, leading to increased awareness. In addition, high background radiation areas have been mapped out for safety measures. Such areas include, Mrima Hill in Kenya (Patel 1991), Guarapari in Brazil (Paschoa, 2000), Yangjiang in China, which has been designated as controlled area (UNSCEAR, 2000; Wei et al., 1993), among others.

In India, Sharma et al. (2016) conducted a research on natural radionuclides and radon exhalation rate in cement, as well as its radiological relevance. Gamma ray spectroscopy was used to assess the activity concentration of primordial radionuclides, radon-226, uranium-238, potassium-40 and thorium-232, while CAN technique was applied in determination of the rate of radon exhalation. Radium equivalent for assorted flooring materials was also determined and the results compared. The obtained values were determined below the maximum permissible value at  $370 \text{ Bqkg}^{-1}$  (UNSCEAR, 1988), with the black granite registering the lowest radium equivalent at  $23.49 \text{ Bqkg}^{-1}$ , in comparison to the orange marble at  $202.63 \text{ Bq kg}^{-1}$ . The difference in the radium equivalent values could be associated with the activity levels of  $^{232}\text{Th}$  and  $^{40}\text{K}$ .

Njinga and Tshivhase (2016) evaluated natural radionuclide concentration as well as the outdoor gamma dose rate in the environs of Tudor shaft gold mines in South Africa. The authors further determined the radionuclide levels in the internal organs in cattle from the area, in addition to calculating the lifetime cancer risk. The activity concentration of  $^{232}\text{Th}$ ,  $^{40}\text{K}$  and  $^{238}\text{U}$  were determined as  $47 \pm 3.7 \text{ Bqkg}^{-1}$ ,  $87 \pm 5.1 \text{ Bqkg}^{-1}$  and  $271 \pm 3.6 \text{ Bqkg}^{-1}$ , respectively. The outdoor gamma dose rate ranged from  $131 \pm 5.4 \text{ nGy/h}$  to  $202 \pm 14 \text{ nGy/h}$ , while average annual effective dose in the environs of the study area was determined to be above the global mean at  $(0.16-0.25) \text{ mSv/y}$ . The internal organs of cattle from the study area were found to contain very high heavy metals and uranium content in comparison to a control group. For instance, the uranium levels were 4000 times higher than that of the control group. This observation was attributed to presence of both artificial and natural radionuclides from the mining process. The lifetime cancer risk was estimated at two to three times above the global mean (Njinga and Tshivhase, 2016).

In the artisanal gold mines of Awwal in Nigeria, Girrigisu et al. (2014) assessed the radiological levels in soils using a NaI(Tl) detector. The obtained activity levels and their corresponding hazard indices were found to be within permissible limits, thus didn't pose significant health risk.  $^{40}\text{K}$  had the highest activity concentration at  $425 \pm 5.6 \text{ Bq kg}^{-1}$ , followed by  $^{226}\text{Ra}$  ( $23 \pm 2.01 \text{ Bq kg}^{-1}$ ), and  $^{232}\text{Th}$  ( $19 \pm 1.2 \text{ Bq kg}^{-1}$ ). The annual effective dose rate was  $0.042 \text{ mSv/year}$ , compared to the UNSCEAR (1993) benchmark at  $0.07 \text{ mSvyr}^{-1}$ . Likewise, Ademola et al. (2015) conducted a similar study around the gold mines of Itaganmodi. The mean activity levels for  $^{238}\text{U}$ ,  $^{40}\text{K}$ , and  $^{232}\text{Th}$  were determined at  $55 \pm$

1.2 Bq kg<sup>-1</sup>, 505 ± 7.1 Bq kg<sup>-1</sup> and 26 ± 2.7 Bq kg<sup>-1</sup>, respectively and 8.7 ± 1.8 Bq kg<sup>-1</sup>, 102 ± 12 Bq kg<sup>-1</sup> and 17 ± 2.6 Bq kg<sup>-1</sup> respectively, in the surrounding residential areas. The annual effective dose was above the global mean at 81.3 µSv y<sup>-1</sup>. Local variations in activity levels were exhibited in the study, which could be associated with the kind of the geology of gold bearing rocks (Ademola et al., 2015).

Uosif et al. (2015) investigated the activity levels of natural radionuclides <sup>40</sup>K, <sup>232</sup>Th and <sup>226</sup>Ra, and their corresponding hazard indices in granites and quartz-bearing gold, in addition to chemical analyses. Radionuclide concentration was determined using sodium iodide detector and chemical analyses using XRF spectroscopy. The specific activity was determined at <sup>232</sup>Th (6 ± 0.7 to 42 ± 2 Bq kg<sup>-1</sup>), <sup>226</sup>Ra (3 ± 0.5 to 43 ± 2 Bq kg<sup>-1</sup>) and <sup>40</sup>K (128 ± 6 to 682 ± 35 Bq kg<sup>-1</sup>). Total effective dose rate of 16 – 70 mSv y<sup>-1</sup> and absorbed dose rate of (13 – 58) nGy h<sup>-1</sup> were recorded.

Mangala (1987) conducted an elemental analyses study in Mrima Hill, Coastal Kenya, from which he established high elemental concentration levels of rare earths and thorium. Patel (1991) also undertook a follow up study to determine the environmental radioactivity. Very high dose levels comparable to those of areas classified as high background radiation areas were recorded in this area. For instance, external gamma radiation dose as high as 1375 mRem/yr, which is fifty times the background values were recorded.

Ghiassi-nejad (2002), found that residents of Ramsar city in Iran, which is a HBRA were exposed to radiation doses of 10.3 mGy/y. The maximum dose recorded was 260 mSv/y. These two studies attributed the high radiation levels to local geology. Incidentally, the inhabitants of these areas locally source their construction materials such as soils and rocks, thus continuously exposing the residents to potentially greater radiation risks.

Patel et al. (2012) conducted a radiological study in Lambwe area, south-western Kenya. The area was established to be a high background radiation area, with maximum absorbed dose levels of 6100 nGy/h and a mean of 2113 nGy/h being recorded. The author attributed the high doses to local geology that is predominantly carbonatites. He further noted that the study area is in a high-altitude region, thus contribution of cosmic radiation to the absorbed dose could be significant.

Omari (2013) carried out a comparable study in Kerio Valley in Rift valley, Kenya. This region has been associated for long with high radioactivity levels. He noted that even

though the values were above the global mean, they were however within the permissible levels. The author further investigated various types of rocks like quartzite, granite and tuff for radioactivity. Quartzite exhibited indoor and outdoor dose levels above the global mean (60 nGy/h) at 157 nGy/h and 159 nGy/h respectively. But, in a different part of the Kerio valley region, Nderitu et al. (2001), reported low annual effective dose levels, at 0.091 mSv/yr.

Patel et al. (2011) conducted a radiological study, to evaluate the degree of exposure of gold miners in Migori, Western Kenya, to radionuclides and dust. The absorbed dose rate of between 17 and 177 nGy h<sup>-1</sup> and an average of 42 nGy/h, was reported. This was below the global mean of 60 nGy/yr. In the neighbouring Homa mountains, Otwoma et al. 2012 evaluated the radioactivity and dose levels in soil and rock samples. The radionuclide activity levels were high at; <sup>232</sup>Th (409 Bq kg<sup>-1</sup>), <sup>226</sup>Ra (195 Bq kg<sup>-1</sup>) and <sup>40</sup>K (915 Bq kg<sup>-1</sup>), as compared to global mean at <sup>232</sup>Th (30 Bq kg<sup>-1</sup>), <sup>226</sup>Ra (35 Bq kg<sup>-1</sup>) and <sup>40</sup>K (400 Bq kg<sup>-1</sup>). The outdoor absorbed dose rate at 1m distance above the ground was determined at 108 to 1596 nGy/h. The annual effective dose varied between 28 μSv/h to 1681 μSv/h, and a mean of 470 μSv/h. As a result of the high radiation levels, Homa mountains can be classified as a high background radiation area (Otwoma et al. 2012).

Kinyua et al. (2001), did a study to assess the extent of radiation exposure to the miners as well as local community in Kisii county in Kenya which has the biggest soapstone mines such as Tabaka quarries. Activity concentrations for <sup>226</sup>Ra, <sup>40</sup>K and <sup>232</sup>Th, in addition to associated radiation hazard indices were determined. The mean absorbed dose was determined nine times the global average, at 541.4 nGy/h. The external and internal hazard index was above the recommended value. Therefore, there is concern over suitability of soapstone as a construction material and for sculpture making.

Osoro et al. (2011) carried out a baseline study on radionuclide concentrations in surface soils in residential areas/ villages around two proposed titanium mines in Coastal Kenya, prior to commencement of the mining process. The study served as a reference for future radiological monitoring studies, once the mining process commences. The author further used the obtained activity concentrations to calculate absorbed dose rate in air. The activity concentration for <sup>40</sup>K, <sup>226</sup>Ra and <sup>232</sup>Th were below global mean as well as those obtained from similar studies in other parts of Kenya at  $77 \pm 15$  Bq kg<sup>-1</sup>,  $20 \pm 4.8$  Bq kg<sup>-1</sup> and  $28 \pm$

5.8 Bq kg<sup>-1</sup> respectively. Similarly, the calculated dose rate was lower than global mean at 29 nGy/h.

A research carried out by Hashim et al. (2004) offers an intriguing perspective about the origin of <sup>137</sup>Cs along the Kenyan coast. In this particular study, the author looked into artificial and natural radionuclide concentrations in the sediments. HPGe detector was used to identify the radionuclides present in the sediments. The study revealed low level contamination of <sup>137</sup>Cs. Presence of <sup>137</sup>Cs was a puzzle due to absence of any nuclear facilities in Kenya. He pointed out towards the possibility of these nuclides being transported from other areas, although further research is necessary. The obtained effective dose varied from 0.02 to 0.19 mSv/y, far below the recommended limit (ICRP, 1991).

#### **2.4 Environmental Impact of Gold Mining**

Occurrence of gold deposits in Kilimapesa, Narok county is good and timely news for Kenya. It will contribute towards the country's socio-economic development agenda, as well as in diversifying the economy of the local communities. However, there is a downside to these development; environmental degradation. Some of the most significant environmental concerns resulting from gold mining include; change in land-use patterns, land degradation, deterioration of flora and fauna, and impact on both surface and underground water sources as well as the drainage system (Erraiyan, 2014; Bhumika, 2014). Above all, elevation of metal content of soil and water resources is a key concern (Pereira *et al.*, 2008; Angelovičová and Fazekašová, 2014). The significance and magnitude of these effects on the environment depend on size and scale of exploration activities, in addition to topography, climatic conditions, nature of mineral deposits, method of mining, among others (MoEF, 2007).

Contamination of agricultural soils and water resources with heavy metals is a major challenge associated with mining (Humsaand Srivastava, 2015). For instance, during the pre-processing stage, minerals are ground into fine particles that are more mobile. The particles can easily be carried away by wind or water over long distances, with potential of contaminating not only the nearby lands but also those that are miles away. In addition, the metals can find their way into river systems or even seep downwards polluting underground water.

## CHAPTER THREE: METHODOLOGY

### 3.1 Overview

The procedures used in this study for sample collection, preparation, instrumentation and analyses are outlined in this chapter. A detailed discussion of radiation indices used as an indicator for human exposure will be discussed.

### 3.2 Sampling: Description of the Study Area

The sampled study area is located in the Kilimapesa gold mining block in Lolgorian region, Narok County. The area is a block of 65 square kilometres. The sampled points were selected randomly within the mining block as shown on figure 3.1 (b).



Figure 3.1(a) : Kenyan map indicating the Kilimapesa mining area in Lolgorian, Source: <http://www.goldplat.com/projects/kilimapesa-gold-kenya>

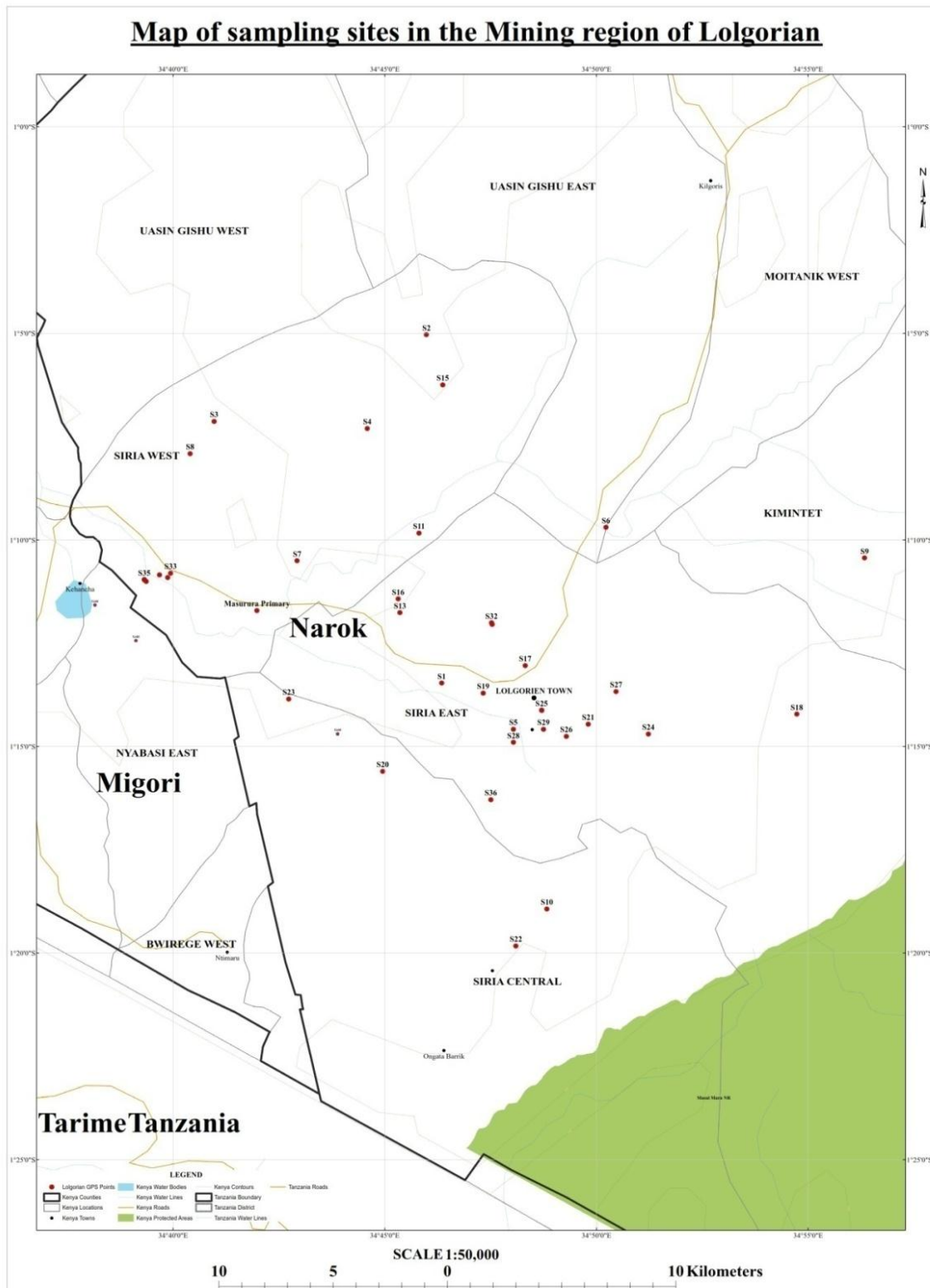


**Fig 3.1(b): A map showing the mining blocks sampled in Lolgorian.**

### **3.3 Sampling**

A total of thirty-six 36 sampling sites were identified for soil sampling. Soil samples were collected at a depth of 10 - 20 cm. For each sampling sites, three subsamples were obtained within a radius of 1m. The three subsamples were homogenized in situ, to obtain a representative sample of about 0.5 kg, which was kept in well labeled polythene bags for transportation to the laboratory for preparation and analyses.

### **3.4 Sample Preparation for Radioactivity Measurements and Trace Elements Determination.**

The samples were initially air dried for two weeks, followed by oven drying at a temperature of 60 °c – 80 °c to constant weight. The samples were then ground to break down aggregates. Grinding helps not only in size reduction, but also in ensuring homogeneity of the elements in the sample.

For radioactivity analyses, about 300 g of the pulverized samples were sealed in 200 cc plastic containers for a period of one month prior to gamma analyses. This was to give the samples time to attain secular equilibrium between gaseous radon and its short-lived daughters ( $^{214}\text{Bi}$  and  $^{214}\text{Pb}$ ) and the long-lived precursor radionuclides.

For EDXRF analyses, the samples were further pulverized using a pestle and mortar and sieved using a 60  $\mu\text{m}$  sieve. Portions of sieved soil samples were then diluted with starch binder in ratios of 1:4 (20%) and thoroughly mixed to homogeneity. Three pellets, each weighing approximately 350 mg were prepared using a hydraulic press from each sample for heavy metal analysis.

### **3.5 Instrumentation of HpGe Gamma Spectroscopy and measurements**

For radiation detection, different types of detectors e.g. filled detectors (scintillation counters, ionization chamber, Geiger-Muller counters, and proportional counters), scintillation or semiconductor detectors, can be used. The basic principle for all these radiation detection techniques is generation of an electrical signal once the radiation interacts with the active volume of the detector (Knoll, 1999). HPGe detector is a one of the most sensitive and efficient radiation detection instrument, this type of detector was used for radiation analyses during this study.

Germanium and silicon are some of the most commonly used semiconductor materials in radiation detection. Detectors made from ultra-pure germanium material are usually

referred to as hyper-pure germanium (HpGe) or intrinsic detectors (Knoll, 1999). Detection and measurement of gamma radiation usually necessitates a thick depletion layer i.e. a greater sensitive volume (Cember, 2009). At the moment, HpGe detector is popularly used for detection of gamma radiation. Figure 3.2 gives a schematic representation of gamma ray spectroscopy used in this study. In general, the unit is made up of HpGe detector, multichannel analyser (MCA), amplifier (AMP), PC and at times a printer. The HPGe detector is a coaxial geometry, relative efficiency of 30%.

Measurement of activity of the NORMs in soil samples was done with HPGe gamma spectrometer (figure 3.2). Samples were run for 12 hours. In addition, the environmental background radiation was assessed using an empty container, prior to sample measurements. The background measurements were done for each sample to correct for net peak intensities of radionuclides of interest.



**Figure 3.2: The HpGe gamma spectrometer at the Institute of Nuclear Science & technology (INST)**

From the obtained gamma photo-peaks in the  $^{232}\text{Th}$ - series,  $^{238}\text{U}$  equivalent decay series, and in  $^{40}\text{K}$  series, their respective activity concentrations were evaluated. For instance, the  $^{232}\text{Th}$  activity concentration was obtained from the mean intensities of  $^{228}\text{Ac}$  and  $^{212}\text{Pb}$ , while  $^{238}\text{U}$  activity concentrations were calculated from the mean intensities of the  $^{214}\text{Bi}$  and  $^{214}\text{Pb}$  (Mohanty *et al.*, 2004) at the respective nuclide energies shown in table 3.1

Calibration of the HPGe system is essential in acquiring accurate results (Gilmore & Hemingway, 1995). This ensures that the acquired spectra are accurately interpreted in terms of energy and specific activity. It is achieved by performing three key tasks; peak width calibration, energy calibration, and efficiency calibration, using high quality standard spectra of appropriate geometry and source matrix (Gilmore & Hemingway, 1995). In this particular study, IAEA standard reference materials; RG-U, RG-K, RG-Th and Soil-375 were used, Energy calibration was done using SRM-1 1332 Kev and 1172 Kev energy line of  $^{60}\text{Co}$ ,  $^{241}\text{Am}$  59.54 Kev and  $^{137}\text{Cs}$  - 661.66 Kev lines

The activity concentrations of the NORMs in the sample were calculated by applying equation 3.1 following evaluation of nuclide spectral line intensities using Oxford PCA3 v.1 software was used for peak deconvolution. The software performs simultaneous fitting and identification to all the significant photo-peaks in the spectra and displays menu driven reports that included centroid channel energy, FWHM of identified peak, net peak area, background counts, intensity and percentage margin of uncertainty.

$$\frac{A_s M_s}{I_s} = \frac{A_r M_r}{I_r} \quad (3.1)$$

Where:  $M_r$  and  $M_s$  is the mass of the reference and sample respectively,  $I_r$  and  $I_s$  are the intensity of reference and sample respectively;  $A_r$  and  $A_s$  is the activity of reference and sample, respectively.

**Table 3.1: Recommended energy lines for gamma-ray emitters of environmental samples (IAEA, 2003)**

Radionuclide	Isotope(s)	Spectral line (KeV)
K- 40	$^{40}\text{K}$	1460.81
Th- 232	$^{212}\text{Pb}$	238.63
	$^{228}\text{Ac}$	911.21
U-238 ( $^{226}\text{Ra}$ )	$^{214}\text{Pb}$	351.92
	$^{214}\text{Bi}$	609.31

In determining the detection limits (DL) for the radionuclides, equation 3.2 was used, whereby the gamma-ray spectral data corresponding to the IAEA calibration standards RG-U, RG-Th and RG-K were used.

$$DL = \frac{3C\sqrt{Bg}}{PA} \quad (3.2)$$

Where:  $B_g$  is the background counts obtained from a gamma peak; PA is the net area under respective gamma photo peaks; C is the activity concentration of the specific radionuclide of interest (in Bq/Kg).

### 3.6 Radiological Data Analyses

Determination of the various radiation hazard indices was done using existing models.

The values obtained from the models for the various indices were then compared to UNSCEAR permissible limits and relevant conclusions made.

From the activity concentrations obtained from this study, the potential radiological hazards were determined. The activity concentrations of the radionuclides were evaluated from their respective gamma ray lines or gamma ray lines emitted from their decay products (Table 3.1). 1460.8 keV spectral line was used to determine  $^{40}\text{K}$ , while the mean activity spectral lines of 238 keV ( $^{212}\text{Pb}$ ) and 911 keV ( $^{228}\text{Ac}$ ) were used to determine  $^{232}\text{Th}$  concentration, and the gamma lines of 609 keV ( $^{214}\text{Bi}$ ) and 351 keV ( $^{214}\text{Pb}$ ) were used to calculate  $^{226}\text{Ra}$  concentration. On the other hand, radiological hazards due to  $\gamma$ -ray radiation were assessed using radium equivalent activity ( $R_{\text{eq}}$ ), Gamma index ( $I_{\text{yr}}$ ) and external hazard index ( $H_{\text{ex}}$ ; Bashir et al., 2012).

#### 3.6.1 Radium equivalent

Natural soil samples contain primordial radionuclides to varying degrees. The index used to calculate the associated potential radioactive hazards is the Radium Equivalent. To model radium equivalent an assumption that 4810 Bq  $\text{kg}^{-1}$  of potassium-40, 259 Bq  $\text{kg}^{-1}$  of thorium-232 and 370 Bq  $\text{kg}^{-1}$  of Uranium-238 have equivalent dose (Kolo et al. 2015; Dabayneh et al. 2008) . Equation 3.3 is used to calculate radium equivalent.

$$R_{\text{eq}} = A_{\text{U}} + 1.43 A_{\text{Th}} + 0.077 A_{\text{K}} \quad (3.3)$$

Where  $A_{\text{u}}$ ,  $A_{\text{th}}$  and  $A_{\text{k}}$  are the activity concentrations of uranium-238, thorium-232 and potassium-40 respectively.

### 3.6.2 Gamma Index

It is an index used as an indicative radioactive hazard potential associated with the materials.

$$I_{yr} = \frac{1}{150}A_U + \frac{1}{100}A_{Th} + \frac{1}{1500}A_K \quad (3.4)$$

Where  $A_u$  is the activity concentration of uranium-238,  $A_{th}$  the activity concentration of thorium-232 and  $A_k$  the activity concentration of potassium-40.

### 3.6.3 External Hazard Index

External hazard index and internal hazard index are used to limit the required dose rate annually to  $1 \text{ mSv y}^{-1}$ , the model is outlined by Beretka & Mathew (1985)

$$H_{ex} = \frac{A_U}{370} + \frac{A_{Th}}{259} + \frac{A_K}{4810} \quad 3.5 \text{ (a)}$$

Where:  $A_{Th}$ ,  $A_U$  and  $A_K$  is the specific activities of  $^{232}\text{Th}$ ,  $^{238}\text{U}$  and  $^{40}\text{K}$  respectively.

On the other hand, internal hazard index is evaluated using the equation

$$H_{in} = \frac{A_U}{185} + \frac{A_{Th}}{259} + \frac{A_K}{4810} \quad 3.5 \text{ (b)}$$

### 3.6.4 Absorbed dose

The absorbed dose rates in air (D) were estimated from the obtained activity concentration  $^{40}\text{K}$ ,  $^{232}\text{Th}$  and  $^{238}\text{U}$ , using equation 3.6 (UNSCEAR 1993).

$$D = 0.427A_U + 0.662 A_{Th} + 0.043A_K \quad (3.6)$$

$A_{Th}$ ,  $A_U$  and  $A_K$  is the specific activities of  $^{232}\text{Th}$ ,  $^{238}\text{U}$  and  $^{40}\text{K}$  respectively

### 3.6.5 Annual Effective Dose

The annual effective dose (E) due to NORMs was calculated by applying equation 3.7 (UNSCEAR, 1993). An outdoor occupancy factor (f) of 0.4 and a dose conversion coefficient (Q) of  $0.7 \text{ Sv Gy}^{-1}$  was used to convert the absorbed dose rate in air to the effective dose were used (UNSCEAR, 2000).

$$E = T f Q D \quad (3.7)$$

Where; T = total seconds per year.

### 3.7 EDXRF Elemental Analyses

In this study, Amptek Experimenters' Kit X-123 SSD spectrometer was used. The spectrometer consists of the X-ray tube for sample excitation with collimators, to focus X-rays on the crystal and detector and a Si(Li) detector. The equipment was operated at 30 KV and 80  $\mu$ A.

The samples were measured in air and irradiated for 50 seconds. The obtained spectra were evaluated for intensities by non-linear least square fitting software called AXIL (Analysis of X-Ray Spectra Interactive Least Square Fitting) and QAES (Quantitative Analysis of Environmental Sample) software from the IAEA.

To validate the analytical procedure, certified reference materials (CRM) were used, and detection limits determined. For this particular study, river clay CRM from IAEA was prepared and analyzed in a similar way as the samples.

The lower limit of detection is the concentration equivalent to three standard counting errors of a set of measurements of the background intensity (Bertin, 1970; Jenkins and Gilfrich, 1992). In this study, the lower limit of detection was determined from measurement of a standard reference PTXRF-09 and the values calculated by using equation 3.8.

$$LLD = \frac{3C\sqrt{R_b}}{P} \quad (3.8)$$

Where:  $R_b$  is the background area of the element;  $P$  is the peak area of the element; and  $C$  is the concentration of the element in  $\text{mg kg}^{-1}$ .

## CHAPTER FOUR: RESULTS AND DISCUSSION

### 4.1 Overview

The results of the radioactivity measurements are presented and discussed in this chapter, in addition to the results for the elemental analyses of the samples. Results for the validation of the analytical methods used will also be presented.

### 4.1 Activity Concentration

HpGe gamma spectrometer operating at a resolution ranging from 2.2 -2.6 keV at FWHM was used for measurements of radioactivity in the soil samples, following sample measurements for 12 hrs, the obtained activity concentrations were subsequently used to determine various radiation hazard indices.

To calculate the activity concentration of the samples, comparative method previously discussed in section 3.5 was used in which the radionuclide spectral intensities for each soil sample and that of the standard references were used. The three standard references used are IAEA-RGTh-1, IAEA-RGK-1 and IAEA-RGU-1, for thorium,  $^{40}\text{K}$ , and uranium radionuclides respectively. . Figure 4.1 shows the gamma spectra obtained for standard references.

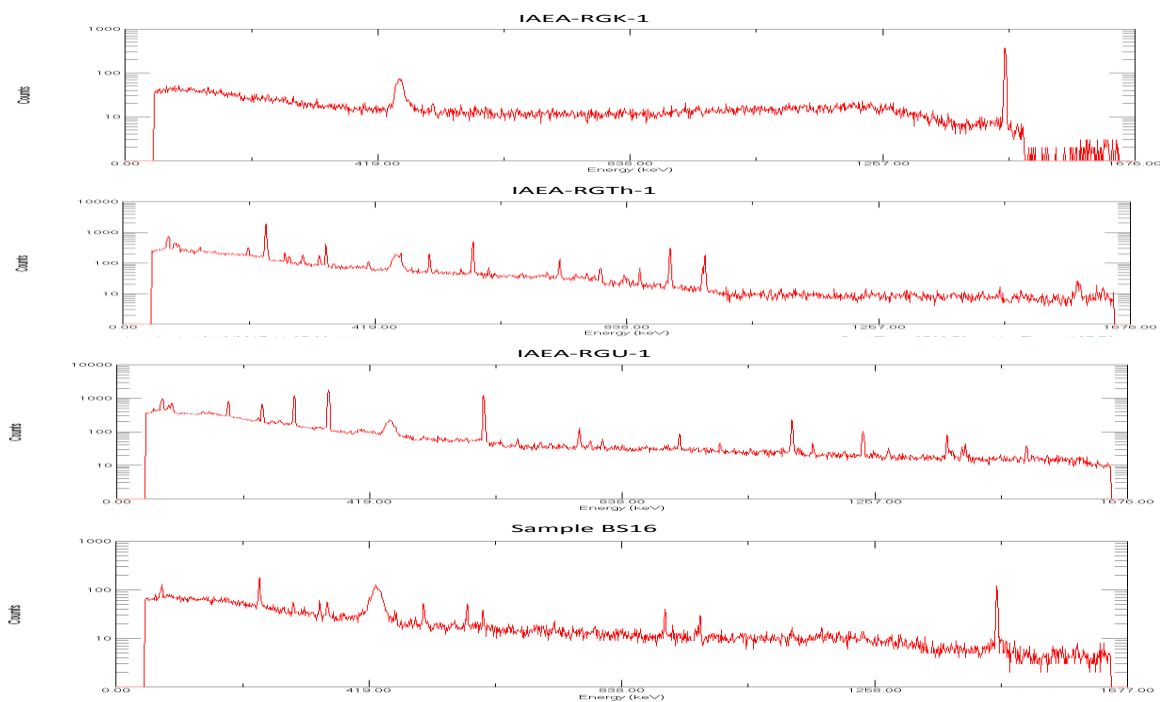


**Figure 4.1: Spectral data for the certified references and a typical sample**

Since the method involves direct comparison of the intensities of the radionuclides in the reference standard to that of the sample effectively minimizes matrix effects such as self-attenuation, coincidence summation etc. and half-life correction will cancel out. The effects due to density are minimized by adoption of similar geometry as that used for measurements for both reference material and the sample.

To achieve the best estimate of the activity concentration, a weighted mean analysis is employed for activity determination; use of at least two discrete gamma-ray lines from the same decay series thereby ensuring a significant reduction in the statistical uncertainty of the derived activity concentrations.  $^{232}\text{Th}$  activity concentration was determined from the average concentrations of  $^{212}\text{Pb}$  and  $^{228}\text{Ac}$  in the samples, while that of  $^{238}\text{U}$  equivalent was determined from the average concentrations of the  $^{214}\text{Pb}$  and  $^{214}\text{Bi}$  decay products (Mohanty *et al.*, 2004).

**Table 4.1: Certified reference material activity concentrations and detection limits; IAEA-RGTh-1, IAEA-RGU-1 and IAEA-RGK-1 respectively**

Radionuclide	Certified Activity conc.	Certified range	Detection limits
$^{232}\text{Th}$ (Bqkg <sup>-1</sup> )	3250	3160-3340	30
$^{238}\text{U}$ (Bqkg <sup>-1</sup> )	4940	4910-4970	5
$^{40}\text{K}$ (Bqkg <sup>-1</sup> )	14,000	13600-14400	5

In general,  $^{40}\text{K}$  was found to be the greatest contributor to radiation exposure in the study area with a mean activity concentration of  $427 \pm 227$  Bq kg<sup>-1</sup>, as compared to  $^{232}\text{Th}$  and  $^{238}\text{U}$  at  $116 \pm 69$  Bq kg<sup>-1</sup> and  $33 \pm 22$  Bq kg<sup>-1</sup>, respectively. While the activity concentration of  $^{238}\text{U}$  was within the reported global mean of 35 Bqkg<sup>-1</sup>,  $^{40}\text{K}$  and  $^{232}\text{Th}$  radionuclides were determined at levels slightly above the global mean of 400 Bq kg<sup>-1</sup> and 30 Bq kg<sup>-1</sup> (UNSCEAR, 2000).

Table 4.2 presents a summary of the activity concentrations of the 36 samples measured in terms of mean, minimum and maximum concentrations, while figure 4.2 shows variations in activity concentrations in the soil samples for this study.

**Table 4.2: Summary of the obtained activity concentrations in Bqkg<sup>-1</sup>**

Descriptive statistics	<sup>40</sup> K	<sup>238</sup> U	<sup>232</sup> Th
Average	427	33	116
Standard deviation	227	22	69
Minimum	64	5	19
Maximum	1084	107	248

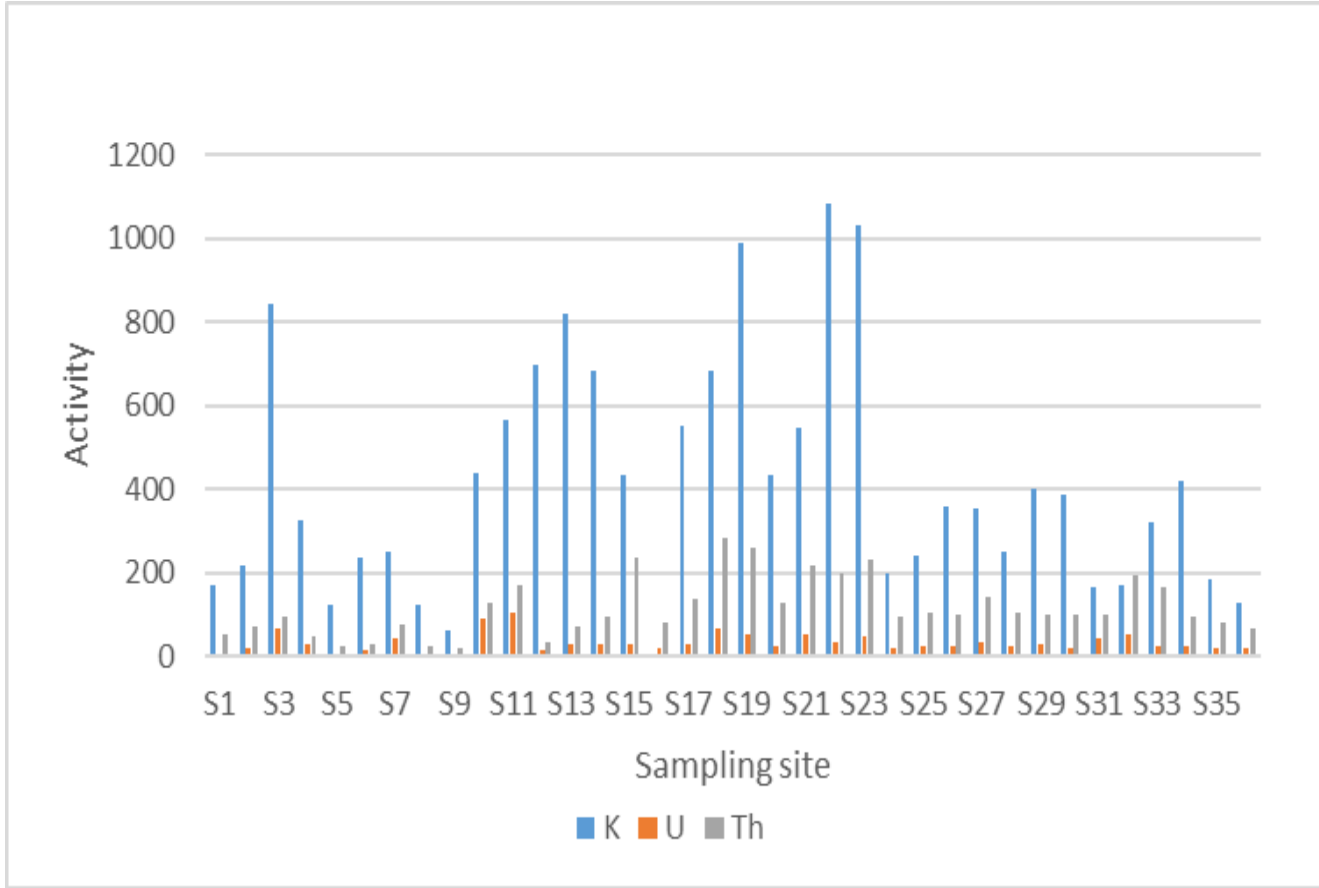


**Figure 4.2: Sample wise distribution of activity concentration due to <sup>238</sup>U, <sup>232</sup>Th and <sup>40</sup>K from measured samples.**

Generally, the three radionuclides i.e.  $^{232}\text{Th}$ ,  $^{238}\text{U}$  and  $^{40}\text{K}$  were randomly distributed in the study area. For instance,  $^{40}\text{K}$  activity concentration ranged between 1084 Bq kg<sup>-1</sup> at site S22 to 64 Bq kg<sup>-1</sup> at site S9, with an average of  $427 \pm 116$  Bq kg<sup>-1</sup>. For  $^{232}\text{Th}$ , the highest activity concentration was reported at site S18 (284 Bq kg<sup>-1</sup>), while the lowest activity being recorded at site S9 at 19.7 Bq kg<sup>-1</sup>. Comparatively lower activity concentrations were reported for  $^{238}\text{U}$ , ranging between 5 – 107 Bq kg<sup>-1</sup>. Similar observation was made by Harb et al. (2014), where great variability in activity concentrations was recorded over a distance of few meters. This observation could be attributed to difference in physical, chemical and geochemical properties of the samples (Assie et al., 2016).

The results obtained in soil samples are within the global average activity concentration set at of 400 Bq kg<sup>-1</sup>, 35 Bq kg<sup>-1</sup>, and 30 Bq kg<sup>-1</sup>, for  $^{40}\text{K}$ ,  $^{232}\text{Th}$  and  $^{238}\text{U}$  radionuclides (UNSCEAR, 2000). These values are however lower than some values reported in similar environments. A study by Patel et al. (2011) in Migori gold mines, Western Kenya, to assess the degree of exposure to miners determined the mean activity concentrations at 409.5 Bqkg<sup>-1</sup> for  $^{232}\text{Th}$ , 195.3 Bqkg<sup>-1</sup> for  $^{238}\text{U}$  and  $^{40}\text{K}$  at 915.6 Bqkg<sup>-1</sup>. The values were comparable to those obtained by Girrigisu et al. (2014), in the artisanal gold mines of Awwal in Nigeria, where the highest mean activity concentration was recorded for  $^{40}\text{K}$  at  $425 \pm 5.6$  Bqkg<sup>-1</sup>, followed by  $^{238}\text{U}$  ( $23 \pm 2.01$  Bqkg<sup>-1</sup>), and  $^{232}\text{Th}$  ( $19 \pm 1.2$  Bqkg<sup>-1</sup>). Likewise, Ademola et al. (2015) in a similar study around Itagunmodi gold mines reported the mean activity levels for  $^{238}\text{U}$ ,  $^{40}\text{K}$ , and  $^{232}\text{Th}$  at  $55 \pm 1.2$  Bqkg<sup>-1</sup>,  $505 \pm 7.1$  Bqkg<sup>-1</sup> and  $26 \pm 2.7$  Bqkg<sup>-1</sup>, respectively.

Figure 4.3 shows the relative abundance of NORMs in the soil samples. About 74 % of the total measured activity concentrations was contributed by  $^{40}\text{K}$ ; 5% by  $^{238}\text{U}$  and 20% by  $^{232}\text{Th}$ . Similar observation was made by Kabasa (2015), where  $^{40}\text{K}$  was found to be the most abundant at  $973 \pm 401$  Bq kg<sup>-1</sup> (90%), followed by  $^{232}\text{Th}$  at  $69 \pm 28$  Bq kg<sup>-1</sup> (6%) , and finally  $^{238}\text{U}$  at  $40 \pm 15$  Bq kg<sup>-1</sup> (4%). The high potassium concentrations can be attributed to the presence of potassium bearing minerals; biotite, muscovite, orthoclase, microcline, feldspars, radioactive minerals; smectite, kaolite. (Okeyode & Ganiyu, 2009). The level of  $^{232}\text{Th}$  reported may be associated to the geology of the area. However, for a definite conclusion, it is necessary to undertake a detailed geochemical survey.

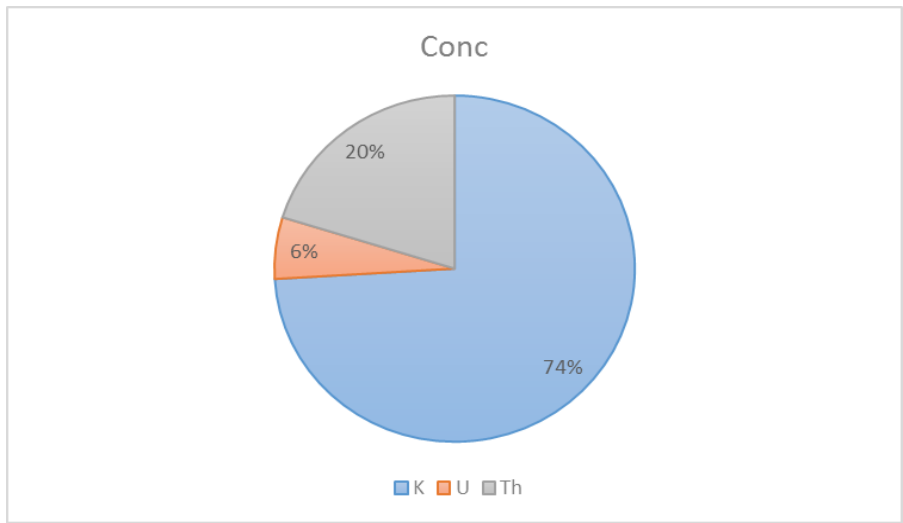


**Figure 4.3: Relative abundance of the radionuclides in soils**

There is a strong correlation between  $^{238}\text{U}$  and  $^{232}\text{Th}$  in the soil samples analyzed in this study

Fig. 4.4, 4.5 & 4.6 shows the correlation between the radionuclides  $^{40}\text{K}$ ,  $^{232}\text{Th}$  and  $^{238}\text{U}$

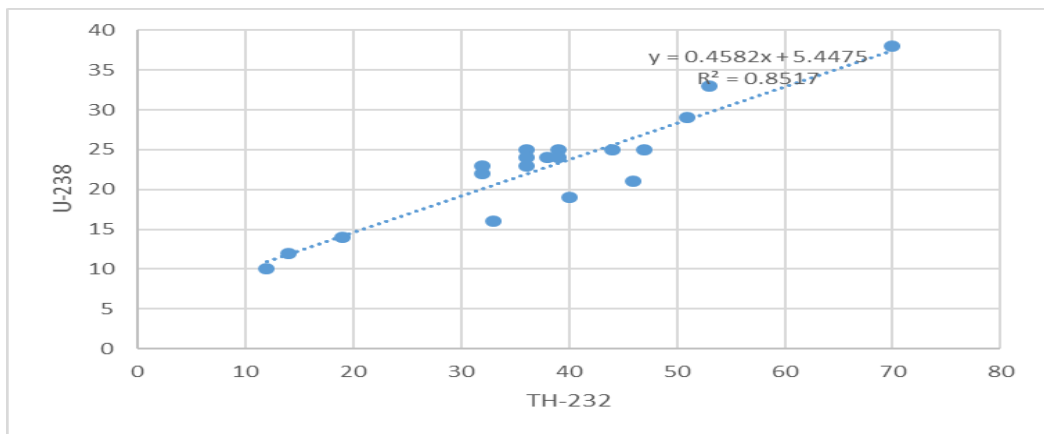


**Figure 4.4: Correlation between the activity concentration of  $^{238}\text{U}$  and  $^{232}\text{Th}$ .**

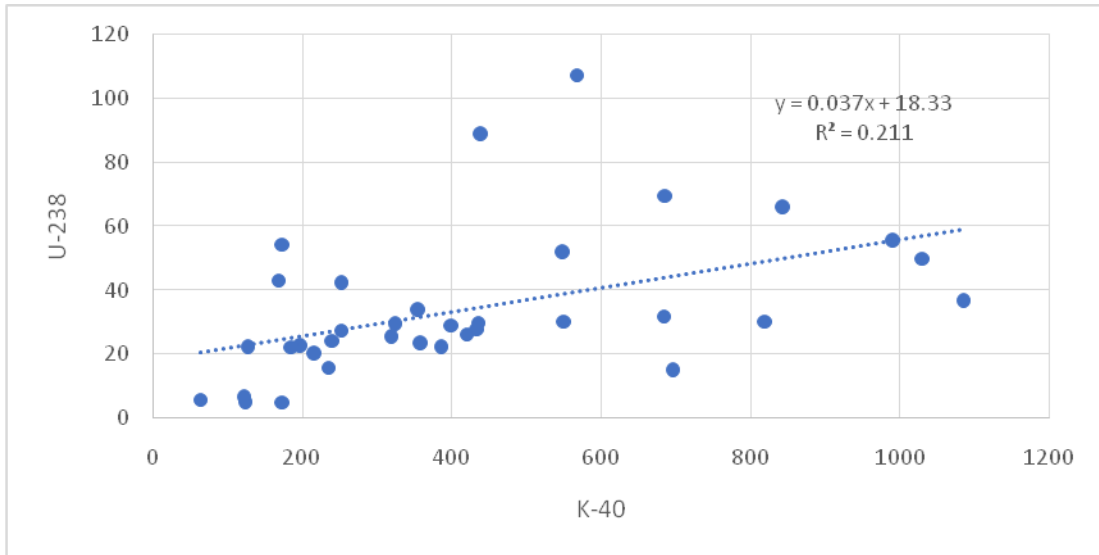


**Figure 4.5: Correlation between the activity concentration of  $^{238}\text{U}$  and  $^{40}\text{K}$ .**

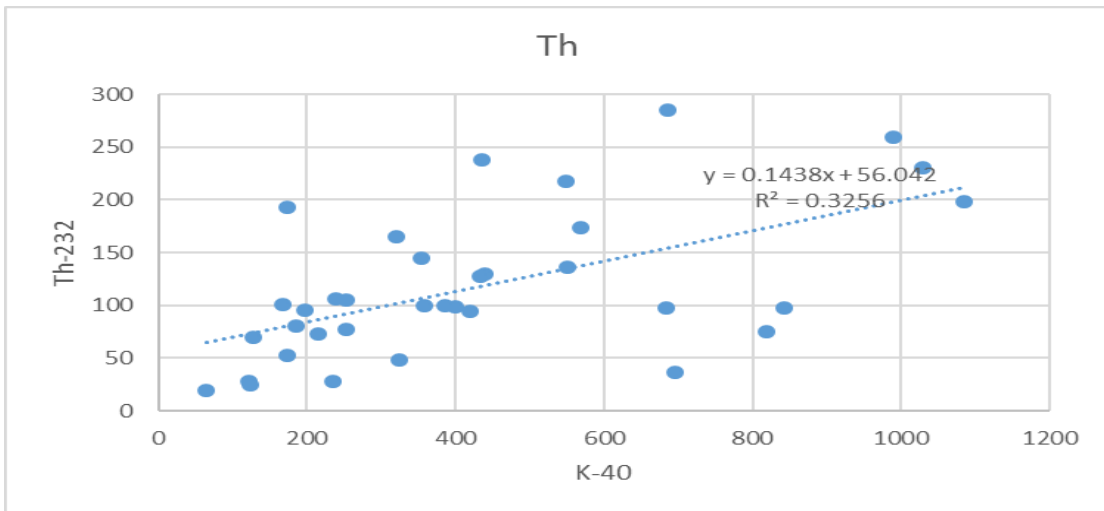


**Figure 4.6: Correlation between the activity concentration of  $^{40}\text{K}$  and  $^{232}\text{Th}$**

#### 4.2 Radiation Hazard Indices

Various indices were applied in the determination of potential radiological risks due to  $\gamma$ -ray radiation. These include, Gamma index ( $I_{\gamma r}$ ), radium equivalent activity ( $Ra_{eq}$ ), external and internal hazard, annual effective dose and absorbed dose rate. Table 4.3 shows a summary of these indices in the samples analyzed in this study. These indices are calculated based on the obtained activity concentrations of the NORMs as presented in table 4.2.

The radium equivalent values were found to range between 128 – 529 Bq kg<sup>-1</sup>, with an average of 232 ± 38 Bq kg<sup>-1</sup>, which is above the world average of 160 Bq kg<sup>-1</sup>, but within the acceptable limit of 350 Bq kg<sup>-1</sup> (UNSCEAR, 2000)..

**Table 4.3: Calculated radiation hazard indices**

Descriptive statistics	R <sub>eq</sub> (Bq kg <sup>-1</sup> )	I <sub>yr</sub>	H <sub>ex</sub>	H <sub>in</sub>	Dr	E
<b>Mean</b>	232	1.66	0.62	0.72	103	0.25
<b>Stdev</b>	38	0.28	0.11	0.12	17	0.04
<b>Max</b>	529	3.77	1.43	1.62	232	0.57
<b>Min</b>	128	0.91	0.34	0.39	56	0.14

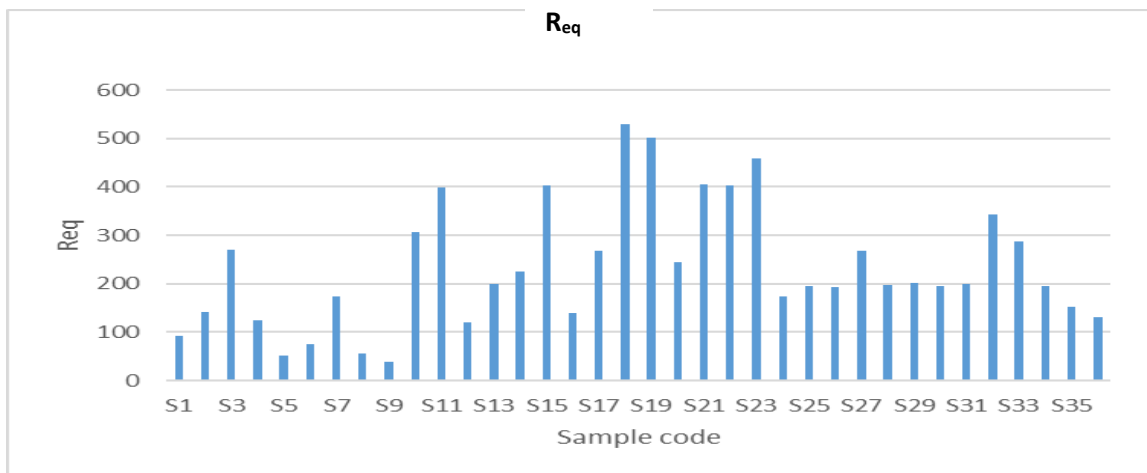


**Figure 4.7: Variation of radium equivalent in the samples**

Gamma radiation index (I<sub>yr</sub>) is used as a screening parameter for materials for possible radiation health effects. In this study, a mean of 1.66 ± 0.28 is reported. The average exceeds the dose criteria where the value of gamma of than less than one (≤1), to correspond to an annual effective dose of ≤1 mSv (Ravisankar et al. 2014).

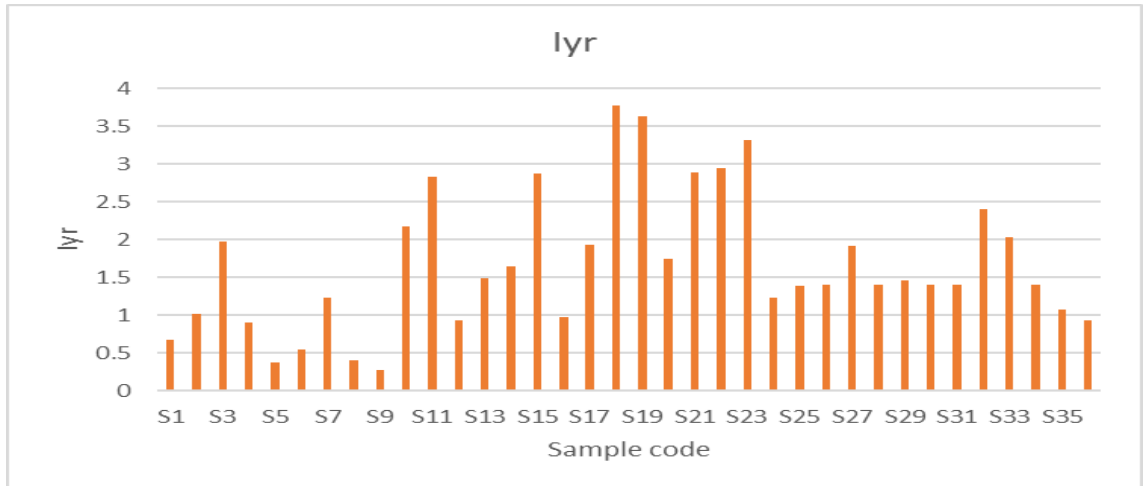


**Figure 4.8:** shows the variation of gamma index in the samples

Internal ( $H_{in}$ ) and external ( $H_{ex}$ ) hazard indices are used to quantify the risks of internal and external exposure to gamma radiation. According to UNSCEAR (2000), a value of the index less than unity is considered insignificant.

Fig 4.9 shows the variation of  $H_{ex}$  and  $H_{in}$  in the samples in which the obtained mean values is  $0.62 \pm 0.11$  and  $0.72 \pm 0.14$  for  $H_{ex}$  and  $H_{in}$  respectively, can then be concluded that the radionuclides do not pose any significant risk.

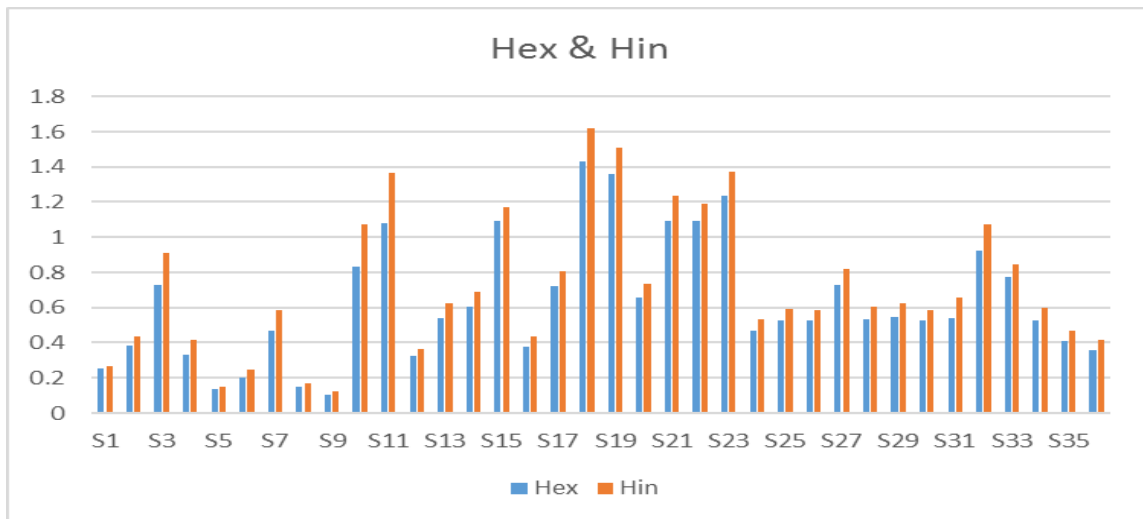


**Figure 4.9:** Variation of  $H_{ex}$  &  $H_{in}$  in the samples

The absorbed dose rates (DR) due to gamma radiations were estimated on assumption that  $^{226}\text{Ra}$ ,  $^{232}\text{Th}$  and  $^{40}\text{K}$  are uniformly distributed, and that other radionuclides contribute insignificantly to the total environmental background dose (Leung et al. 1990; Jacob et al. 1986). The obtained values ranged between 19 nGy/h and 156 nGy/h in the samples fig

(4.10). These values were further applied in calculation of the annual effective dose with an assumption of outdoor occupancy factor of 0.4. An average of  $0.14 \pm 0.04 \text{ mSv/y}$  (Fig 4.11) was recorded against the non-occupation exposure limit of  $1 \text{ mSv y}^{-1}$ , which is below the global mean value of the annual effective dose set at  $0.5 \text{ mSv y}^{-1}$  and a range of  $0.3 - 0.6 \text{ mSv yr}^{-1}$  for individual countries (Senthilkumar et al., 2010; UNSCEAR, 2000).

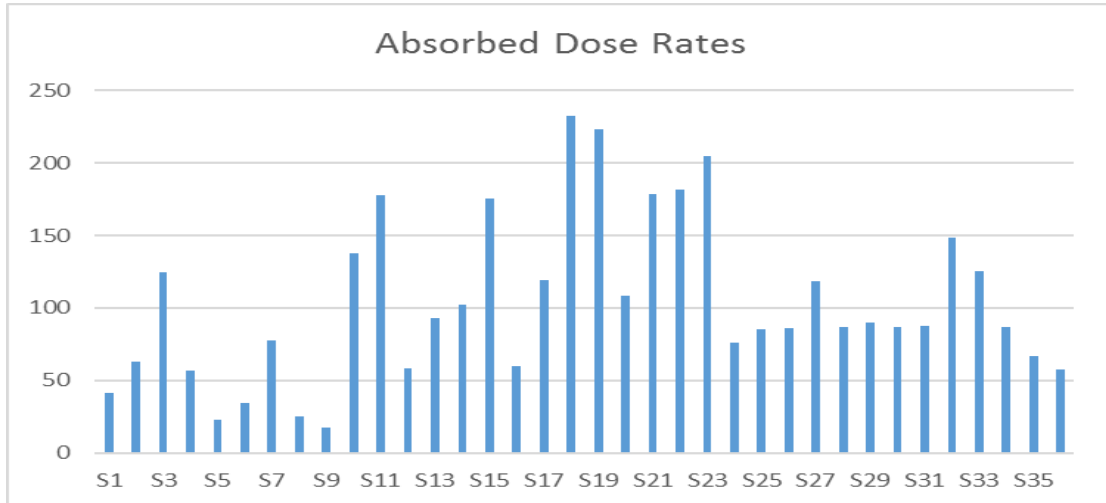


**Figure 4.10: Variation of absorbed dose rates in the samples**

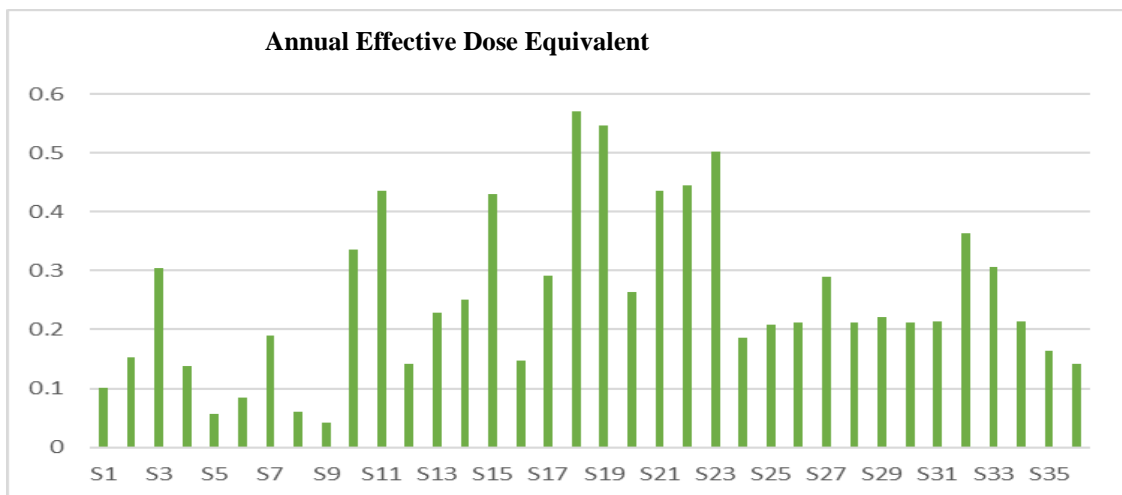


**Figure 4.11: Variation of annual effective dose equivalent in the samples**

### 4.3 Elemental Concentrations

Elemental content of the soil samples from Lolgorian gold mines was determined using Energy Dispersive X-ray Spectroscopy (AMPTEK Experimenter’s Kit). To validate the

analytical method, certified reference material; IAEA-PTXRF-09, from International Atomic Energy Agency was analyzed for comparison of the results of measurement (Table 4.4). Preparation and analytical procedure similar to that of the samples was employed. The obtained experimental results were comparable to the certified values, as presented in table 4.4.

**Table 4.4: Results of the analyses of IAEA-PTXRF09 certified reference material**

<b>Element</b>	<b>Experimental value</b>	<b>Certified value</b>	<b>Certified range</b>
<b>K</b>	(1.78 ± 0.29) %	(1.95 ± 0.11) %	(1.84 – 2.06) %
<b>Ca</b>	(1.29 ± 0.09) %	(1.38 ± 0.10) %	(1.28 – 1.48) %
<b>Fe</b>	(3.01 ± 0.14) %	(2.97 ± 0.15) %	(2.82 – 3.12) %
<b>Ti</b>	(4286 ± 360) ppm	(4300 ± 290)ppm	(4010 – 4590)ppm
<b>Mn</b>	(1047 ± 87) ppm	(1000 ± 90)ppm	(930 – 1090) ppm
<b>Zn</b>	(93 ± 11) ppm	(96 ± 7.7) ppm	(88.3 – 103.7) ppm
<b>Rb</b>	(114 ± 9.1) ppm	(107 ± 8.4) ppm	(98.6- 115.4) ppm
<b>Zr</b>	(325 ± 24) ppm	(302 ± 20.4) ppm	(281.6 – 322.4) ppm
<b>Pb</b>	(43 ± 7.9)ppm	(36.9 ± 5.1)ppm	(31.8 – 42.0) ppm

Iron is a major constituent in the soil samples analyzed in this study. Concentration ranges of between 1.92 % at site S11 to 30 % at site S36, with a mean concentration of (9.22 ± 7.70) %, are reported. Generally, the iron concentrations in soils are usually high, where concentrations range between (0.5 – 5) % is recorded in uncontaminated soils (Kabata-Pendias and Pendias, 1992). Therefore, these soil are highly enriched with iron, the values are comparable to those obtained by Odumo (2009), in a study in Migori gold mines, Southern Nyanza, Kenya, where iron was determined as the most abundant element at a concentration range of between 10.5 % to 24.5 %.

Titanium and manganese are some of the minor elemental constituents in the soil samples, with mean concentration reported at  $4370 \pm 2500 \text{ mg kg}^{-1}$  and  $1870 \pm 1500 \text{ mg kg}^{-1}$  respectively. The highest Ti concentration level was reported at site S12 ( $11100 \text{ mg kg}^{-1}$ ), while the lowest concentration was recorded at site S6 ( $684 \text{ mg kg}^{-1}$ ). These concentration values are comparable to those reported by Odumo (2009), at between  $171 - 13000 \text{ mg kg}^{-1}$ . However, these values are lower than those reported by Maina et al. (2012), near titanium mine in Kenyan coastal region, where Ti concentration range of (0.13 % to 2.81 %) are reported. Patel and Mangala (1994), reported higher values in their studies conducted in Mrima Hill, Kenya, where Ti was determined as the major constituent with an uneven distribution in the concentration range of 1.00 % to 9.00 % and a mean concentration of 4.69 %, the highest Mn concentration was recorded at site S12 at  $5741 \pm 182 \text{ mg kg}^{-1}$ , while the lowest concentrations at site S19. A strong positive correlation was observed between Ti and Mn concentrations ( $R= 0.74$ ) as shown by table 4.6, whereby both elements reported highest concentrations at site S12 and low concentrations at site S19 and S16. Table 4.5 shows the results of elemental composition in soil samples

**Table 4.5: Elemental Concentrations in soils samples**

<b>Element</b>	<b>Ti (mg kg<sup>-1</sup>)</b>	<b>Mn (mg kg<sup>-1</sup>)</b>	<b>Fe (W%)</b>	<b>Zn (mg kg<sup>-1</sup>)</b>	<b>Rb (mg kg<sup>-1</sup>)</b>	<b>Zr (mg kg<sup>-1</sup>) 1)</b>	<b>Pb (mg kg<sup>-1</sup>)</b>
S1	4641 ± 365	1032 ± 68	5.4 ± 0.1	82 ± 10	115 ± 4.9	515 ± 9.9	37 ± 8.3
S2	6049 ± 406	1193 ± 76	7.2 ± 0.2	83 ± 13	85 ± 4.4	220 ± 6.7	40 ± 7.5
S3	5444 ± 389	1754 ± 89	6.7 ± 0.2	63 ± 15	160 ± 6.2	253 ± 7.5	48 ± 7.2
S4	5789 ± 437	2368 ± 107	6.7 ± 0.1	67 ± 11	119 ± 4	272 ± 7	41 ± 8
S5	3968 ± 513	932 ± 128	26.0 ± 0.4	19 ± 15	25 ± 3	213 ± 7	239 ± 17
S6	684 ± 174	852 ± 58	4.8 ± 0.1	26 ± 8	16 ± 2	144 ± 5	185 ± 10
S7	4695 ± 396	5283 ± 215	8.8 ± 0.2	132 ± 14	117 ± 5	334 ± 8	51 ± 8
S8	989 ± 165	556 ± 54	3.0 ± 0.2	18 ± 9	32 ± 3	144 ± 6	528 ± 32
S9	4630 ± 352	2259 ± 129	12.3 ± 0.3	86 ± 9	39 ± 3.2	78 ± 4	51 ± 7
S10	1433 ± 169	564 ± 56	2.2 ± 0.1	179 ± 16	33 ± 3	141 ± 5	503 ± 29
S11	1671 ± 137	486 ± 36	1.9 ± 0.1	25 ± 5	37 ± 2	206 ± 5	27 ± 5
S12	11100 ± 600	5741 ± 182	21.7 ± 0.3	85 ± 16	147 ± 6	417 ± 11	50 ± 8
S13	5717 ± 350	2264 ± 86	6.3 ± 0.1	39 ± 6	65 ± 3	369 ± 8	27 ± 5
S14	8239 ± 454	5166 ± 173	16.1 ± 0.3	98 ± 14	73 ± 4	124 ± 5	50 ± 8
S15	5944 ± 465	1102 ± 70	5.8 ± 0.1	65 ± 12	125 ± 5	209 ± 7	30 ± 7
S16	9761 ± 423	2533 ± 106	13.6 ± 0.2	792 ± 31	96 ± 5	77 ± 4	444 ± 21
S17	4792 ± 315	1535 ± 98	5.6 ± 0.2	54 ± 11	122 ± 5	260 ± 7	44 ± 8

<b>Element</b>	<b>Ti (mg kg<sup>-1</sup>)</b>	<b>Mn (mg kg<sup>-1</sup>)</b>	<b>Fe (W%)</b>	<b>Zn (mg kg<sup>-1</sup>)</b>	<b>Rb (mg kg<sup>-1</sup>)</b>	<b>Zr (mg kg<sup>-1</sup>)</b>	<b>Pb (mg kg<sup>-1</sup>)</b>
S18	7334 ± 410	4248 ± 175	14.9 ± 0.3	181 ± 18	100 ± 4	157 ± 5	320 ± 16
S19	1703 ± 201	377 ± 37	2.4 ± 0.1	71 ± 10	30 ± 2	148 ± 5	714 ± 27
S20	1344 ± 148	510 ± 42	1.9 ± 0.1	13 ± 5	26 ± 2	110 ± 4	20 ± 4
S21	5804 ± 502	3033 ± 150	18.0 ± 2.0	227 ± 16	33 ± 3	80 ± 5	40 ± 8
S22	3943 ± 281	1523 ± 82	5.2 ± 0.1	41 ± 12	105 ± 4	182 ± 5	31 ± 7
S23	1886 ± 209	805 ± 72	2.9 ± 0.2	127 ± 16	37 ± 3	139 ± 5	642 ± 35
S24	1860 ± 228	882 ± 83	4.2 ± 0.3	137 ± 16	52 ± 4	253 ± 9	594 ± 39
S25	1411 ± 158	650 ± 54	3.4 ± 0.1	115 ± 13	30 ± 3	157 ± 6	366 ± 22
S26	4951 ± 334	4201 ± 148	7.0 ± 0.1	82 ± 15	126 ± 5	372 ± 9	28 ± 7
S27	4713 ± 336	839 ± 65	4.6 ± 0.1	59 ± 10	133 ± 5	182 ± 8	30 ± 7
S28	782 ± 139	432 ± 41	2.3 ± 0.1	31 ± 8	19 ± 2	89 ± 5	238 ± 12
S31	5751 ± 333	3053 ± 156	11.0 ± 0.2	222 ± 17	70 ± 3	168 ± 6	126 ± 11
S32	3776 ± 552	1079 ± 138	27.3 ± 0.4	22 ± 14	24 ± 3	178 ± 7	233 ± 14
S33	4879 ± 361	1699 ± 96	6.3 ± 0.2	72 ± 14	156 ± 6	253 ± 7.5	45 ± 7
S34	4327 ± 492	2613 ± 120	13.5 ± 0.3	111 ± 18	32 ± 3	87 ± 4	39 ± 8
S35	3614 ± 486	1148 ± 140	30.0 ± 0.5	40 ± 6	19 ± 3	143 ± 6	206 ± 15
S36	4713 ± 336	839 ± 65	4.6 ± 0.1	59 ± 10	133 ± 5	182 ± 5	30 ± 7

Zirconium was determined within moderate levels in all the samples analyzed in this study, and ranges between 77 – 515 mg kg<sup>-1</sup> with a mean of 202 ± 102 mg kg<sup>-1</sup>. These values are comparable to the values of Mrima Hill reported by Patel and Mangala (1994), at between 94 mg kg<sup>-1</sup> and 720 mg kg<sup>-1</sup> and a mean of 251 mg kg<sup>-1</sup>. The values were however lower than those reported by Maina et al. (2012), in a study around a titanium mine at a range of 280 mg kg<sup>-1</sup> to 3300 mg kg<sup>-1</sup>, with a mean of 1190 mg kg<sup>-1</sup>.

Table 4.6 shows the inter-elemental correlation matrix. Zirconium distributions correlate strongly to those of rubidium ( $r=0.57$ ). Zinc, rubidium and lead were also determined above detection limits in all samples. Zinc concentrations ranged between 20 – 792 mg kg<sup>-1</sup>, with an average of 102 mg kg<sup>-1</sup>. These values are lower than those reported by Odumo (2009), at a range of 580 mg kg<sup>-1</sup>, in Migori gold mines, western Kenya. For Rb, a mean of 74 ± 47 mg kg<sup>-1</sup> was recorded in these samples, the reported values were comparable to those obtained by Odumo (2009), at below 100 mg kg<sup>-1</sup>. Rb was found to correlate strongly with Ti ( $R = 0.62$ ), and weakly with Mn ( $r = 0.41$ ). Lead is a non-essential metal in human physiology and can be toxic even at low concentrations, a concentration value of between 20 – 714 mg kg<sup>-1</sup> and a mean of 180 mg kg<sup>-1</sup> were recorded in this study. The mean Pb concentrations reported were higher than those reported globally in surface soils at 35 mg kg<sup>-1</sup> and in varying ranges from 10 to 70 mg kg<sup>-1</sup> (Wuana & Okieimen, 2011), however the concentration is lower than the value reported by Odumo (2009), at a mean of 1473 mg kg<sup>-1</sup>.

**Table 4.6: Inter-element Correlation matrix**

Variables	Ti	Mn	Fe	Zn	Rb	Sr	Zr	Pb
Ti	<b>1</b>							
Mn	<b>0.74</b>	<b>1</b>						
Fe	<b>0.47</b>	<b>0.39</b>	<b>1</b>					
Zn	<b>0.45</b>	0.25	0.09	<b>1</b>				
Rb	<b>0.62</b>	<b>0.41</b>	-0.13	0.10	<b>1</b>			
Sr	-0.10	-0.27	0.05	-0.18	0.12	<b>1</b>		
Zr	0.28	0.28	-0.06	-0.22	<b>0.57</b>	0.17	<b>1</b>	
Pb	<b>-0.40</b>	<b>-0.34</b>	-0.13	0.27	<b>-0.46</b>	-0.01	-0.32	<b>1</b>
<i>Values in bold are different from 0 with a significance level alpha=0.05</i>								

## CHAPTER FIVE: CONCLUSION AND RECOMMENDATIONS

### 5.1 Conclusion

The study assessed the radiological hazards posed to the miners and residents, due to presence of natural radionuclides in soils from Kilimapesa gold mines in Lolgorian-Narok County. To achieve this objective, activity concentration of  $^{40}\text{K}$ ,  $^{232}\text{Th}$  and  $^{238}\text{U}$ , in the soil samples were determined. The obtained radionuclide activity concentrations were used to estimate radiation risks posed, using different radiation hazard indices models. In addition, elemental content of the soil samples was determined.

In general,  $^{40}\text{K}$  was found to be the greatest contributor to radiation exposure in the study area with a mean activity concentration of  $427 \pm 116 \text{ Bq kg}^{-1}$ , as compared to  $^{232}\text{Th}$  and  $^{238}\text{U}$  at  $116 \pm 69 \text{ Bq kg}^{-1}$  and  $33 \pm 22 \text{ Bq kg}^{-1}$  respectively. While the activity concentration of  $^{238}\text{U}$  was within the reported global mean of  $35 \text{ Bq kg}^{-1}$ ,  $^{232}\text{Th}$  and  $^{40}\text{K}$  radionuclides were determined at values slightly above the global mean of  $30 \text{ Bq kg}^{-1}$  and  $400 \text{ Bq kg}^{-1}$ , respectively. The three radionuclides were not uniformly distributed in the study area soils. For instance,  $^{40}\text{K}$  activity concentration ranged between  $64 \text{ Bq kg}^{-1}$  to  $1084 \text{ Bq kg}^{-1}$ , with a mean of  $427 \pm 116 \text{ Bq kg}^{-1}$ , while  $^{238}\text{U}$  ranged between  $5 - 107 \text{ Bq kg}^{-1}$ . This observation could be attributed to difference in physical, chemical and geochemical properties of the samples over small distances.

To assess potential radiological hazards due to gamma radiation, various radiation hazard indices such as radium equivalent activity, gamma index, external and internal hazard index, absorbed dose rate and annual effective dose, were determined. In general the values of these indices although higher than the global averages, indicated that there was no significant radiation risk as a result of NORMs in the study area.

Iron, Ti, Zn, Mn, Zr, Rb and Pb, were determined as the principal constituents in all the sampling sites selected for the study. Iron was the major constituent in the soil samples, followed by Ti and Mn, with a mean concentration of  $9.22 \pm 7.70 \%$ ,  $4370 \pm 2500 \text{ mg kg}^{-1}$ , and  $1869 \pm 1509 \text{ mg kg}^{-1}$  respectively. Mean concentrations below  $100 \text{ mg kg}^{-1}$ , were recorded for Zn, Zr, Rb and Pb.

### 5.2 Recommendations

From the results and conclusions drawn from this study the following are recommended:

- 1) Regular monitoring of radioactivity in Lolgorian;
- 2) To measure the ambient atmosphere absorbed and annual effective dose;
- 3) Analyze radioactivity in water sources; rivers, boreholes, as well as in biological samples.

## REFERENCES

- Ahmad, N., Jaafar, M.S., Bakhsh, M. and Rahim, M., 2015. An overview on measurements of natural radioactivity in Malaysia. *Journal of Radiation Research and Applied Sciences*, 8(1), pp.136-141.
- Ayham A., Abdul-Jabbar A., Awatif S. and Asia H. (2016). Determination of natural radioactivity by gamma spectroscopy in Balad soil, Iraq. *Advances in Applied Science Research*, 7(1): 35 – 41.
- Beretka, J. and Mathew, P.J., 1985. Natural radioactivity of Australian building materials, industrial wastes and by-products. *Health physics*, 48(1), pp.87-95.
- Charles, M., 2001. UNSCEAR Report 2000: sources and effects of ionizing radiation. *Journal of Radiological Protection*, 21(1), p.83.
- Eisenbud, M. and Gesell, T.F., 1997. *Environmental Radioactivity from Natural, Industrial & Military Sources: From Natural, Industrial and Military Sources*. Academic press.
- Ghiassi-Nejad, M., Mortazavi, S.M.J., Cameron, J.R., Niroomand-Rad, A. and Karam, P.A., 2002. Very high background radiation areas of Ramsar, Iran: preliminary biological studies. *Health Physics*, 82(1), pp.87-93.
- Girigisu, S., Ibeanu, I.G.E., Adeyemo, D.J., Onoja, R.A., Bappah, I.A. and Okoh, S., 2014. Assessment of radiological levels in soils from artisanal gold mining exercises at Awwal, Kebbi state, Nigeria. *Research Journal of Applied Sciences, Engineering and Technology*, 7(14), pp.2899-2904.
- Goldplat, assessed on 14April 2016, <http://www.goldplat.com/projects/kilimapesa-gold-kenya>
- Harb S., El-Kamel A. H., Zahran A. M., Abbady A. and Ahmed F. A. (2014). Assessment of natural radioactivity in soil and water samples from Aden governorate South of Yemen

region. *International Journal of Recent Research in Physics and Chemical Sciences*, 1(1): 1 - 7

Hashim, N.O., Rathore, I.V.S., Kinyua, A.M. and Mustapha, A.O., 2004. Natural and artificial radioactivity levels in sediments along the Kenyan coast. *Radiation Physics and Chemistry*, 71(3), pp.805-806.

Kabasa, S.O. (2014) Environmental Radiation Exposure Hazard Associated With Coal Deposits of Mui Basin Block C, Kitui County. M.Sc Thesis, University of Nairobi. Pp 38-42.

Knoll, G.F., 2010. *Radiation Detection and Measurement*. John Wiley & Sons.

Nderitu, S.K., Maina, D.M. and Kinyua, A.M., 2001. Natural gamma radiation levels, indoor and water 222 RN Concentrations in soil division of Kerio valley, Kenya.

Njinga, R.L. and Tshivhase, V.M., 2016. Lifetime cancer risk due to gamma radioactivity in soils from Tudor Shaft mine environs, South Africa. *Journal of Radiation Research and Applied Sciences*.

Odumo, B., Carbonell, G., Angeyo, H.K., Patel, J.P., Torrijos, M. and Martín, J.A.R., 2014. Impact of gold mining associated with mercury contamination in soil, biota sediments and tailings in Kenya. *Environmental Science and Pollution Research*, 21(21), pp.12426-12435.

Odumo, O.B., Mustapha, A.O., Patel, J.P. and Angeyo, H.K., 2011. Radiological survey and assessment of associated activity concentration of the naturally occurring radioactive materials (NORM) in the Migori artisanal gold mining belt of southern Nyanza, Kenya. *Applied Radiation and Isotopes*, 69(6), pp.912-916.

Osoro, M.K., Rathore, I.V.S., Mangala, M.J. and Mustapha, A.O., 2011. Radioactivity in Surface Soils around the Proposed Sites for Titanium Mining Project in Kenya. *Journal of Environmental Protection*, 2(4), p.460.

- Otwoma, D., Patel, J.P., Bartlol, S. and Mustapha, A.O., 2012. Radioactivity and dose assessment of rock and soil samples from Homa Mountain, Homa Bay County, Kenya. In *XI Radiation Physics and Protection Conference, Cairo, Egypt* (pp. 25-28).
- Otwoma, David An investigation of the Radioecology of the Carbonatite deposits in the Homa Mountain region in South Nyanza, Kenya (2012).
- Patel, J.P., 1991. Environmental radiation survey of the area of high natural radioactivity of Mrima hill of Kenya. *Discovery and innovation*, 3(3), pp.31-35.
- Senthilkumar, G., Raghu, Y., Sivakumar, S., Chandrasekaran, A., Anand, D.P. and Ravisankar, R., 2014. Natural radioactivity measurement and evaluation of radiological hazards in some commercial flooring materials used in Thiruvannamalai, Tamilnadu, India. *Journal of Radiation Research and Applied Sciences*, 7(1), pp.116-122.
- Sharma, N., Singh, J., Esakki, S.C. and Tripathi, R.M., 2016. A study of the natural radioactivity and radon exhalation rate in some cements used in India and its radiological significance. *Journal of Radiation Research and Applied Sciences*, 9(1), pp.47-56.
- United Nations Scientific Committee on the Effects of Atomic Radiation *sources, Effects and Risks of Ionizing Radiation* UNSCEAR 2012 Report to the General Assembly
- United Nations. Scientific Committee on the Effects of Atomic Radiation, 2008. *Effects of Ionizing Radiation: Report to the General Assembly, with scientific annexes* (Vol. 1). United Nations Publications.
- Uosif, M.A.M., Issa, S.A. and El-Salam, L.A., 2015. Measurement of natural radioactivity in granites and its quartz-bearing gold at El-Fawakhir area (Central Eastern Desert), Egypt. *Journal of Radiation Research and Applied Sciences*, 8(3), pp.393-398.
- Valentin, J. ed., 2007. *The 2007 Recommendations of the International Commission on Radiological Protection* (pp. 1-333). Oxford, UK: Elsevier.